Åbo Akademi University

Turun yliopisto
University of Turku

Investigation of molecular interactions of prenylflavonoids at $GABA_A$ receptor subtypes

Master's Thesis

University of Turku

MSc Degree Programme in

Drug Discovery and Development

May 2019

Student

Tamara Somborac

Scientific supervisor

Outi Salo-Ahen

Institute of Biomedicine

UNEVERSITY OF TURKU
Institute of Biomedicine, Faculty of Medicine

SOMBORAC, TAMARA: Investigation of molecular interactions of prenylflavonoids at GABAA receptor subtypes
Master's Thesis, 52 p, 1 appendix
Institute of Biomedicine, Drug Discovery and Development
May 2019

Prenylated flavonoids derived from Hops *(Humulus lupulus)* activate the γ-aminobutyric acid (GABA) type A receptors through positive and negative modulation. Currently, these compounds' binding site at the different $GABA_AR$ subtypes is still unknown.

Molecular interactions of several prenylated flavonoids were investigated at different $GABA_AR$ binding sites. The focus was on the receptor subtypes containing αβγ and αβδ subunits and the aim was to identify the most likely binding site for the prenylflavonoids by studying the relation between a ligand structure and the residues defining its putative pocket and the ligand's calculated binding affinity.

Available $GABA_AR$ crystal structures were obtained from the Protein Data Bank, and a comparative model of the $\alpha_6\beta_3\delta$ receptor subtype was built using the MODELLER software. The compounds were docked at the putative binding sites of the studied $GABA_AR$ subtype structures with the GLIDE tool of the Maestro molecular modeling package. An estimate of the free energy of binding was calculated with the Prime/MMGBSA tool of Maestro for all the docked receptor-ligand complexes.

The obtained results suggest that prenylflavonoids may bind to more than one pocket in the extracellular domain of the studied $GABA_AR$ subtypes. It was not possible to distinguish high affinity binding sites from low affinity binding sites as the docking results varied for each compound in the studied pockets. Discrepancy in results is likely caused by modeling binding site without knowing the correct conformations of the side chains forming the pockets. Based on the modelled α6β3δ subtype, β3δ interface may be the most likely binding site for the hops compounds. To determine the binding of the prenylated flavonoids most accurately, experimental structure determination by X-ray crystallography could be attempted.

Key Words: GABA-A, Ligands, Binding Sites, Subunits.

Contents

1.Scientific background of the research project

1.1. $GABA_AA$ receptor

Class A γ-aminobutyric acid (GABA) receptors are abundant in mammalian central nervous system(CNS), but can also be found in other types of tissues, where they are most commonly located postsynaptically (Yocum et al., 2016). They represent the major inhibitory receptors in human brain, potentiated by the endogenous neurotransmitter GABA. The $GABA_A$ receptors get activated and change their conformation after GABA is bound, which results in channel opening and permeation of both chloride and bicarbonate ions. Consequently, the cell membrane becomes hyperpolarized and inhibits the possibility for neuronal transmission (Uusi-Oukari and Korpi, 2010; Miller and Aricescu, 2014). GABA-induced inhibition of neuronal excitation can last for milliseconds or have a longer time range. Postsynaptic receptors confer the short, millisecond-lasting inhibition, whereas extrasynaptically located $GABA_A$ receptors ($GABA_ARs$) mediate long-term inhibition(Sigel and Steinmann, 2012).

Architecture of these cysteine (Cys)-loop type of receptors includes multiple subunits, usually assembled in a pentameric form, with a variety of isoform compositions (Olsen et al., 2009). Subunits are termed α1 to 6, β1 to 3, γ1 to 3, δ, ε, θ, π and ρ1 to 3. All the subunits forming the receptors are placed in the cell membrane in such a manner that they have an extracellular, transmembrane and intracellular domain. The extracellular part of each subunit starts with the N-terminus that continues into alpha helices, beta sheets and the Cys-loops characteristic for this receptor family. Subunits then permeate the cell membrane where they form four alpha-helical M transmembrane domains (M1-M4). The largest loop connecting M3 and M4 domains, located inside the cell plays an important role in phosphorylation and receptor regulation. M4 domain finally exits the lipid bilayer and ends up in the C-terminus back in the extracellular side of the membrane (Figure 1a). The extracellular domain of the receptor is where GABA and benzodiazepine (BZD) agonists bind, between the beta sheets of two different subunits (Figure 1b and 1c) (Clayton et al., 2007; Uusi-Oukari et al., 2010).

The beta sheets of a single subunit assemble into a beta-sandwich form that is comprised of ten β-strands. Numbering of the beta strands starts at the N-terminus and ends at the C-terminus, whereas the annotation of the loops (A to F) begins at the C-terminus and ends at the N-terminus. Loops A to C belong to the outer sheet and they are the principal

plus (+) side of a subunit, while the minus (−) complementary side is comprised of D to F loops. The details of the architecture are presented in Figure 1d. These sheets are named the outer and the inner sheet, meaning that the outer one is localized abluminally and the inner one is luminal (Ernst et al., 2005).

The principal receptor isoform, present in the human brain, is assembled from two α_1 and two β_2 subunits and one γ_2 subunit (Figure 1c). This subunit composition corresponds to the synaptic form of the receptor and generates a fast receptor response and a short inhibition. On the other hand, extra synaptic $GABA_AR$s are believed to contain the δ subunit commonly paired with the α_4 or α_6 subunit (Yakoub et al., 2018).

The subunits that form GABA receptors are highly homologous within the same class, and show relatively good homology among the various subclasses, 60% to 80% and 30% to 40%, respectively (Clayton et al., 2007). Various isoforms of the homologous subunits are important for they define the properties of the receptor, such as ligand affinity, channel opening and conductivity (Cossart et al., 2005). Majority of $GABA_AR$s are assembled from five subunits, forming heteropentamers, with the $\alpha_1\beta_2\gamma_2$ receptor subtype being the most abundant one. The arrangement of this receptor subtype, as well as that of the $\alpha_1\beta_3\gamma_2$ subtype, that is also studied in this project, is shown to be β–α–γ–β–α (Puthenkalam et al., 2016). X-ray structure determination shows that possible interfaces between the subunits in αβγ receptor types are α+/β–, β+/α–, α+/γ–, γ+/β– (Tretter et al., 1997; Baumann et al., 2007; Zhu et al. 2018; Masiulis et al. 2019). It is less clear how δ subunit-containing receptors are arranged; hence the exact interface types are less known. Some of the arrangements in this receptor subtype are determined (Lee et al., 2016), however, no crystal structure of a $GABA_AR$ heteropentamer containing the δ subunit is released to date.

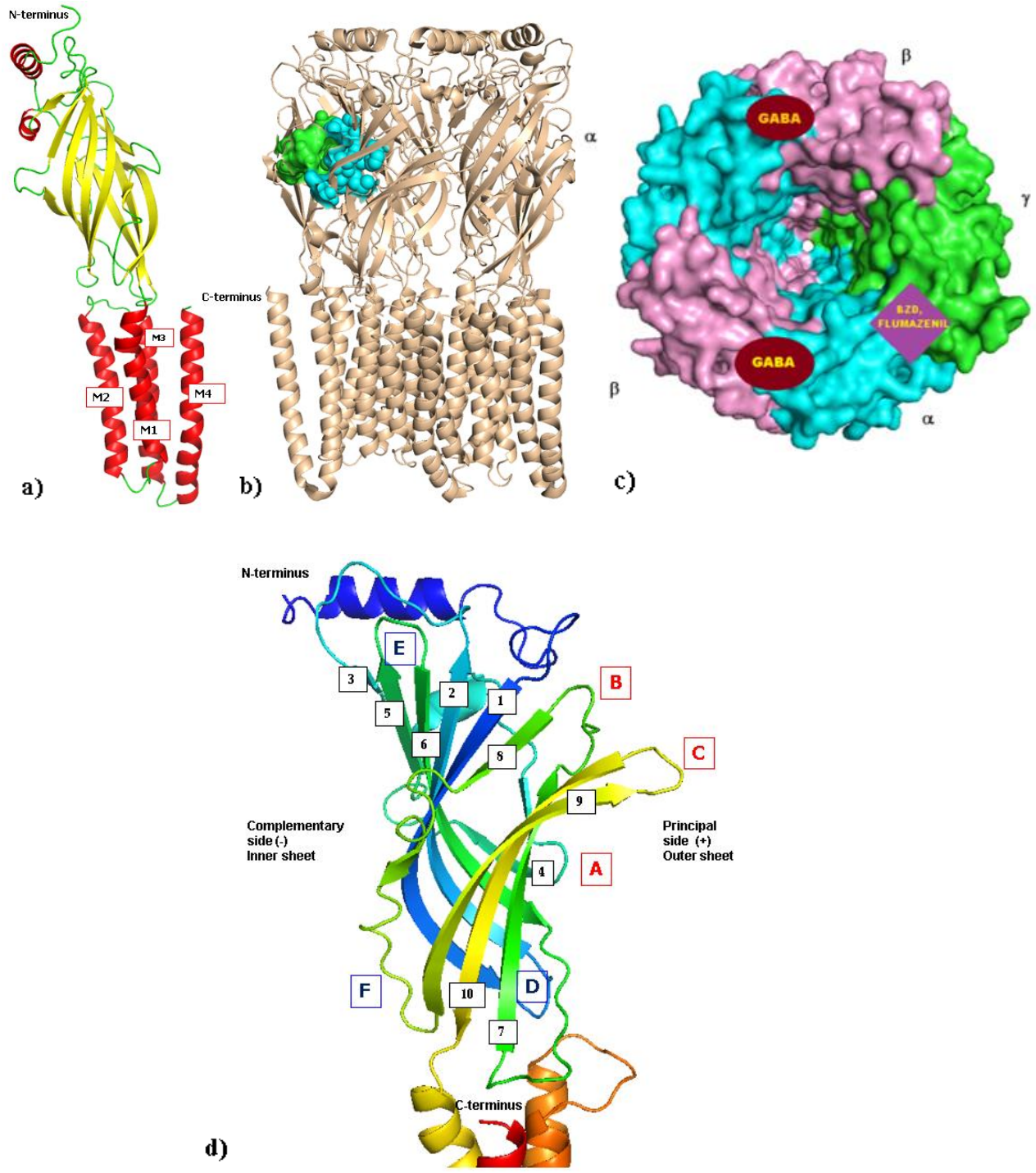

Figure 1. a) Topology of a single subunit of the $GABA_AR$ (cartoon representation). Alpha helices are colored red, beta sheets yellow and loops are shown in green. b) Side view of $GABA_AR$ architecture with a ligand pocket marked with green and blue spheres that represent the residues of the two subunits that form the BZD binding pocket. c) Top view of the receptor (surface presentation) shows the arrangement of the subunits and the binding sites of GABA, benzodiazepine (BZD) and flumazenil. In the place of γ subunit, δ may be present (PDB ID: 6D6U). d) Topology of a single $GABA_AR$ subunit. The beta strands are depicted as cartoon representation and numbered from 1 to 10, starting at the

N-terminus. Loops from A to C, that are part of the principal (+) side are annotated in red and the complementary (− side) loops D to F are annotated in blue (PDB ID: 4COF).

In addition to binding GABA, these receptors are drug targets for compounds that possess sedative and anxiolytic effects. Furthermore, there is evidence from the literature that reduced $GABA_AR$ activity results in disorders such as seizures and epileptic encephalopathies (Macdonald et al., 2004).

Drug classes such as benzodiazepines (BZDs), β-carbolines, Z-drugs (zopiclone, zolpidem) as well as pyrazolo quinolinones exert their effects by allosterically modulating the $GABA_ARs$. On the other hand, a broad range of side effects is believed to result from the Cl^- channel gate altering. It is believed that the difference in the type of the effect caused by the drugs may result from the subunit type and the binding pocket localization involved in the receptor-ligand interaction. For example, experimental evidence shows that sedative effects are mediated by α_1-subunit and this subunit type is also being targeted for sedative and hypnotic effects. On the other hand, memory-affecting receptors are those that include α_5 in their structure, while effects such as anxiolysis are displayed in the α_2 and α_3 subunit containing $GABA_ARs$ (Rudolph et al., 1999).

GABA binds to the extracellular domain (ECD) of the receptor, to the classical neurotransmitter binding site. BZDs bind at sites in close proximity to that of GABA, called the high-affinity benzodiazepine binding site. GABA is known to bind to the β_2/α_1 pocket and BZDs at the α_1/γ_2 interface. BZD antagonist, flumazenil binds at a region close to the GABA pocket, as well. On the other hand, receptor isoforms that contain α_4 or α_6 subunits were shown to be BZD insensitive (Sigel et al., 2018). Other drugs elicit their effects by binding to different domains and subunit interfaces. For example, propofol and volatile anesthetics bind closer to the transmembrane domain (Figure 2). Allosteric binding sites that are not canonical GABA binding sites seem to be a good target for optimizing drug selectivity. Identification and design of highly selective drugs that would target $GABA_AR$ is an ongoing issue. However, the fact that the binding pocket-forming subunits such as α_2, α_3 and γ_2, γ_3 are too similar to each other hampers the precise design of high specificity compounds or those that would have well defined functional selectivity (Sigel et al., 2018).

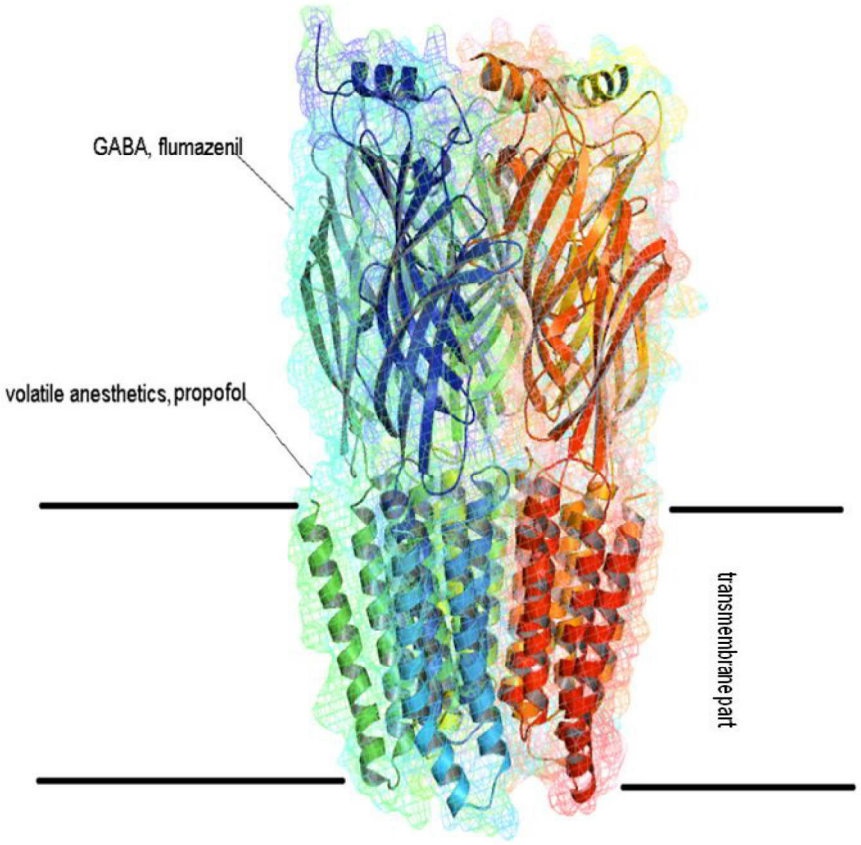

Figure 2. Binding sites of some clinically significant drugs on $GABA_AR$ receptor (PDB ID: 4COF)

1.2. Flavonoids and $GABA_AR$ modulation

In herbal medicine flavonoid compounds derived from hops (*Humulus lupulus*) are used as sleeping aid (Zanoli and Zavatti, 2008) and they also show potential neuroactivity such as alleviating anxiety disorders and affecting the cognition process (Wang et al., 2007, 2011; Zhang et al., 2012; Spencer, 2008, 2009). It is likely that these effects are mediated via $GABA_A$ receptors, the main inhibition site in the brain, via allosteric (or possibly even direct) modulation of the BDZ binding site (Sieghart, 1995; de Oliveira et al., 2018).

Prenylflavonoids in hops extracts, display a wide range of biological activities that are beneficial to human health. The most significant prenylflavonoids are xanthohumol (XN), isoxanthohumol (IXN), and 8-prenylnaringenin (8PN) (Karabín et al., 2016). Evidence from the literature indicates that XN elicited GABAergic effects by modulating $GABA_ARs$ (Aoshima et al., 2006; Sahin et al., 2016). Recently published data regarding the aforementioned hops compounds reveals that prenylflavonoid modulation of the $GABA_AR$ is flumazenil insensitive. This means that the site of action of these compounds

is likely not the same as that of flumazenil (α_1+/γ_2-). Nonetheless, there is some evidence that flavonoids could act through the flumazenil-sensitive site as well (Johnston et al., 2015). The tested hops compounds have the highest affinity for the $\alpha_6\beta_3\delta$ interface (Benkherouf et al., 2019), however, the exact site of action remains unknown.

This study aims to locate the potential binding sites for hops-derived compounds XN, IXN, 8PN and 6-prenylnaringenin (6PN) at $GABA_AR$s and to investigate the interactions between the ligands and the $GABA_AR$ receptor subtypes composed of αβγ and αβδ subunits.

Furthermore, this study focuses on identifying the most likely binding site for the prenylflavonoids through studying the relation between the residues that form a putative binding pocket and the ligand that was docked in it. Additionally, we aim to describe the molecular properties of prenylflavonoids that are important for receptor-ligand interaction and that lead to preference for the binding pocket location. For this, several subunit interfaces are studied. Figure 3 shows the binding pocket where flumazenil was crystallized ($\alpha_1\gamma_2$) and the most important interactions of flumazenil and the residues that form the binding site. Despite the fact that preliminary docking results at the principal isoform ($\alpha_1\beta_2\gamma_2$) show that prenylflavonoids fit well into the flumazenil-binding pocket, this is not the subunit interface that we hypothesize to be the main binding site for them.

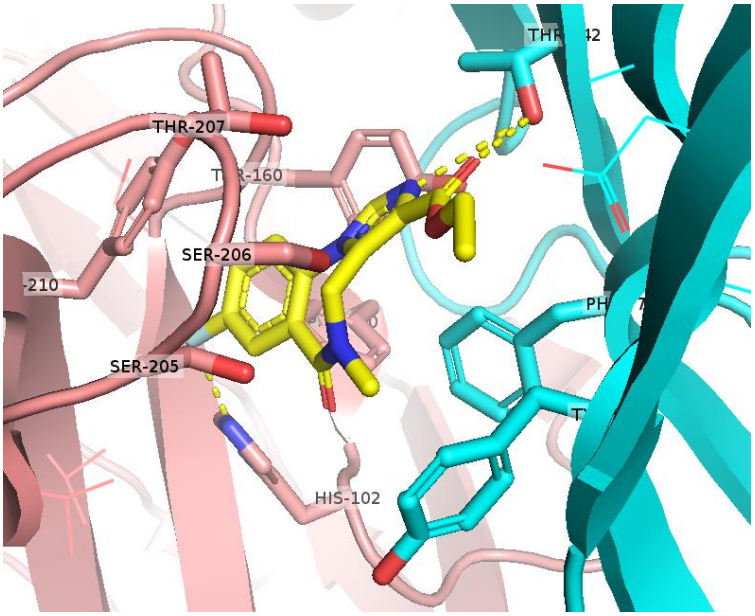

Figure 3. Binding pocket of the $GABA_A$ receptor isoform in which flumazenil was crystallized (PDB ID: 6D6U). Carbon atoms of flumazenil are colored yellow. Subunits α_1 and γ_2 that form the pocket are colored pink and cyan, respectively (all oxygen atoms are in red, nitrogen atoms in blue). The most important interactions are π-π stacking interactions between the diazepine ring of flumazenil and tyrosine 210 and polar (hydrogen bonding) interactions of flumazenil with threonine 142 and histidine 102. Polar interactions are shown as dotted yellow lines.

Despite eliciting GABAergic effects, it is not likely that prenylflavonoids bind to the canonical GABA site on the receptor. Instead, it is likely that binding happens either closer to the transmembrane domain or at another subunit interface that might have similar properties to the flumazenil-binding pocket. This we assume based on the sizes of the molecules (Figure 4) and the ligand-binding pockets of GABA and flumazenil. Flumazenil binds closer to the ECD, and it has some structural similarity to the studied hops compounds; hence, we hypothesize that they are likely to bind at similar pockets.

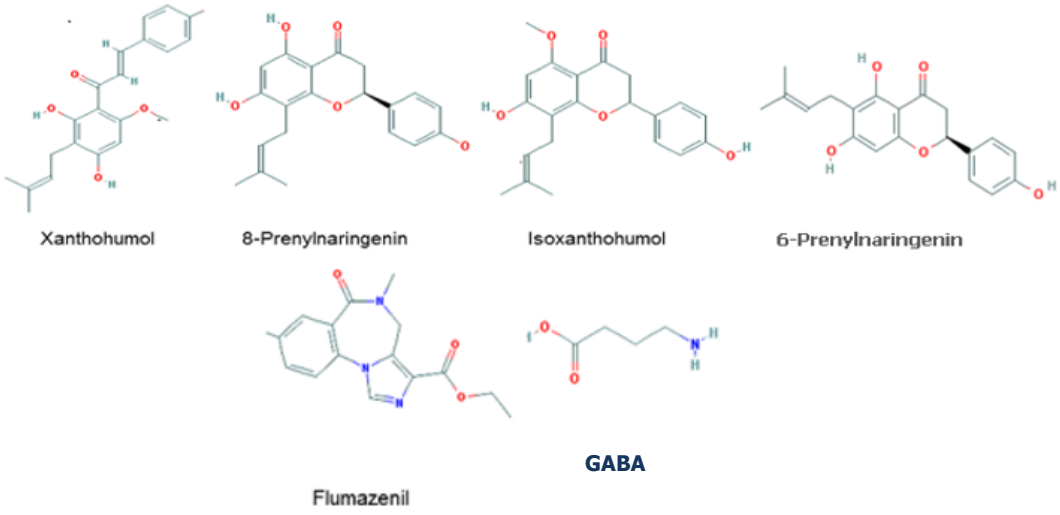

Figure 4. 2D structure of hops-derived compounds, xanthohumol, 8-prenylnaringenin, isoxanthohumol and 6-prenylnaringenin, as well as the BZD antagonist flumazenil and endogenous neurotransmitter GABA.

The ultimate goal of this project is to map the $GABA_A$ receptor subtype properties that mediate the sedative effects of the hops-derived compounds. This would also contribute to understanding the role of different subunits involved in various GABAergic actions in the CNS. Successful determination of the exact site to which our compounds bind would not only help define important binding properties of the molecules but could also help in the rational drug design of more selective $GABA_AR$ ligands that would be devoid of the unwanted effects caused by drugs that act via BZD site such as anxiety, sedation, tolerance and addiction. Additionally, for future prospects, searching for homologous compounds to the tested prenylflavonoid ligands may help identify potential new drugs targeting $GABA_A$ receptor and these compounds could then be tested experimentally. In sum, this research project may not only help identify relevant characteristics of our compounds, but potentially introduce new grounds for creating drugs that possess desirable GABAergic effects and at the same time are do not exert the adverse effects caused by potentiating $GABA_A$ receptor activity.

2. Results

2.1. Homology modeling

The modeling alignments obtained for the subunits α_6 and δ are presented in Figures 5 and 6. The template proteins were selected based on the number of positives and species (*Homo sapiens*) from the Protein BLAST search results (see the Appendix). The BLAST search showed that the B chain of the crystal structure PDB ID: 6D6T and the A chain of the crystal structure PDB ID: 6A96 were the most suitable templates for the α_6 subunit, while the A chain of the crystal structure PDB ID: 6D6T and the A chain of the crystal structure PDB ID: 4COF were the most preferable sequences for creating the 3D model of the δ subunit.

Figure 5. Multiple sequence alignment for the subunit α_6 that was used for creating the homology model.

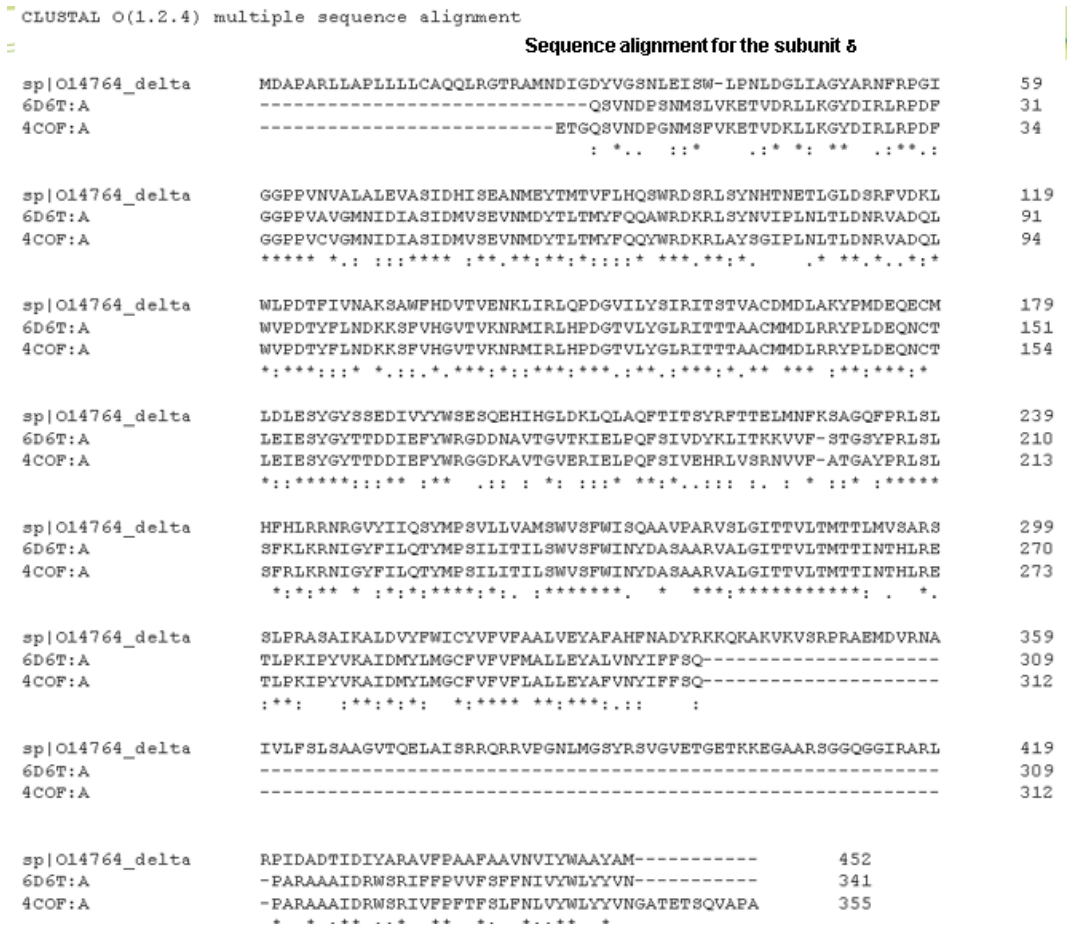

Figure 6. Multiple sequence alignment for the subunit δ that was used for creating the homology model.

The final models for both subunits were selected based on the lowest DOPE-score and visual inspection. Results from the created subunit models are presented in the Figure 7.

a)

Model	molpdf	DOPE score	Model	molpdf	DOPE score
alpha6.B99990001.pdb	8698.14062	-33589.48438	delta.B99990001.pdb	8313.67676	-32069.04297
alpha6.B99990002.pdb	8893.78027	-33183.71094	delta.B99990002.pdb	8418.85840	-31718.07422
alpha6.B99990003.pdb	8810.88867	-33383.23828	delta.B99990003.pdb	8383.19434	-31991.48828
alpha6.B99990004.pdb	8839.62500	-33478.33594	delta.B99990004.pdb	8283.12988	-31871.85547
alpha6.B99990005.pdb	8774.43066	-33304.83594	delta.B99990005.pdb	8297.99707	-31791.06641
alpha6.B99990006.pdb	8705.20215	-33363.91406	delta.B99990006.pdb	8345.70215	-31417.40430
alpha6.B99990007.pdb	8736.67871	-33622.21875	delta.B99990007.pdb	8435.21094	-31471.51953
alpha6.B99990008.pdb	8750.85938	-33085.14453	delta.B99990008.pdb	8420.22559	-31426.65625
alpha6.B99990009.pdb	8759.49219	-33416.39062	delta.B99990009.pdb	8385.50488	-31505.32227
alpha6.B99990010.pdb	8886.80859	-33154.63281	delta.B99990010.pdb	8412.45410	-31963.00391

b)

Model	molpdf	DOPE score	GA341 score
a6b3d.B99990001.pdb	11202.57715	-175694.75000	0.99883
a6b3d.B99990002.pdb	11395.38379	-177316.82812	0.98494
a6b3d.B99990003.pdb	11059.73047	-176203.14062	0.99516
a6b3d.B99990004.pdb	11364.11035	-176447.54688	0.99067
a6b3d.B99990005.pdb	11194.76660	-176839.81250	0.98465
a6b3d.B99990006.pdb	11540.94043	-176552.60938	0.99314
a6b3d.B99990007.pdb	11593.21387	-175669.62500	0.99495
a6b3d.B99990008.pdb	11262.22656	-176612.81250	0.96896
a6b3d.B99990009.pdb	11541.80664	-176187.90625	0.97555
a6b3d.B99990010.pdb	11553.39551	-176645.87500	0.98359

Figure 7. a) Scoring of the created models. In both subunits the lowest DOPE score model was selected. b) Scoring of the final $GABA_AR$ subtype. The lowest DOPE score model was selected for further studies as it seemed the most suitable after visual inspection.

The full receptor model of the $\alpha_6\beta_3\delta$ subtype was then created by employing the Multiple chain model alignment in a similar manner as with the subunits (Sali and Blundell, 1993).

2.2. Molecular dynamics simulations

During the molecular dynamics (MD) simulation the total potential energy of both full receptor model and the binding sites model remained stable (Figure 7). Prior to the MD simulations of the receptor models there was 98.0% and 2.0% residues in favored and allowed regions, respectively, for the full receptor model and 98.0% and 2.0% residues in the favored and allowed regions, respectively, for the binding sites model. There were no residues present in the outlier region for the binding sites model prior to the MD simulation, while for the full receptor model there were 12 residues present in the outlier region. After the MD simulations were completed the Ramachandran analysis of the structures showed 93.2% and 6.4% residues in favored and in allowed regions, respectively, for the binding sites model and 94.4% and 5% for the full receptor model. The first one had four residues (0.4%) in the outlier regions, and the latter had six residues

(0.4%) in the outlier regions. However, neither of those residues were part of any of the studied binding pockets (Figure 8). The crystal structures 4COF and 6D6U did not have any residues in the outlier region and the percentage of the residues I favored and allowed regions in both crystals were 98.0% and 2.0%, respectively.

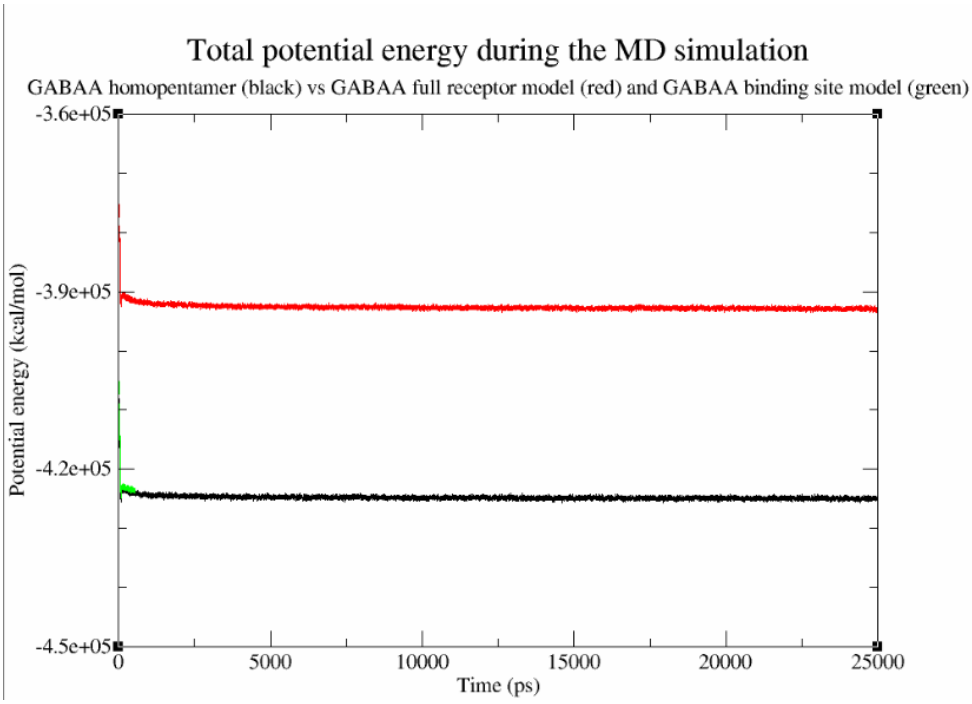

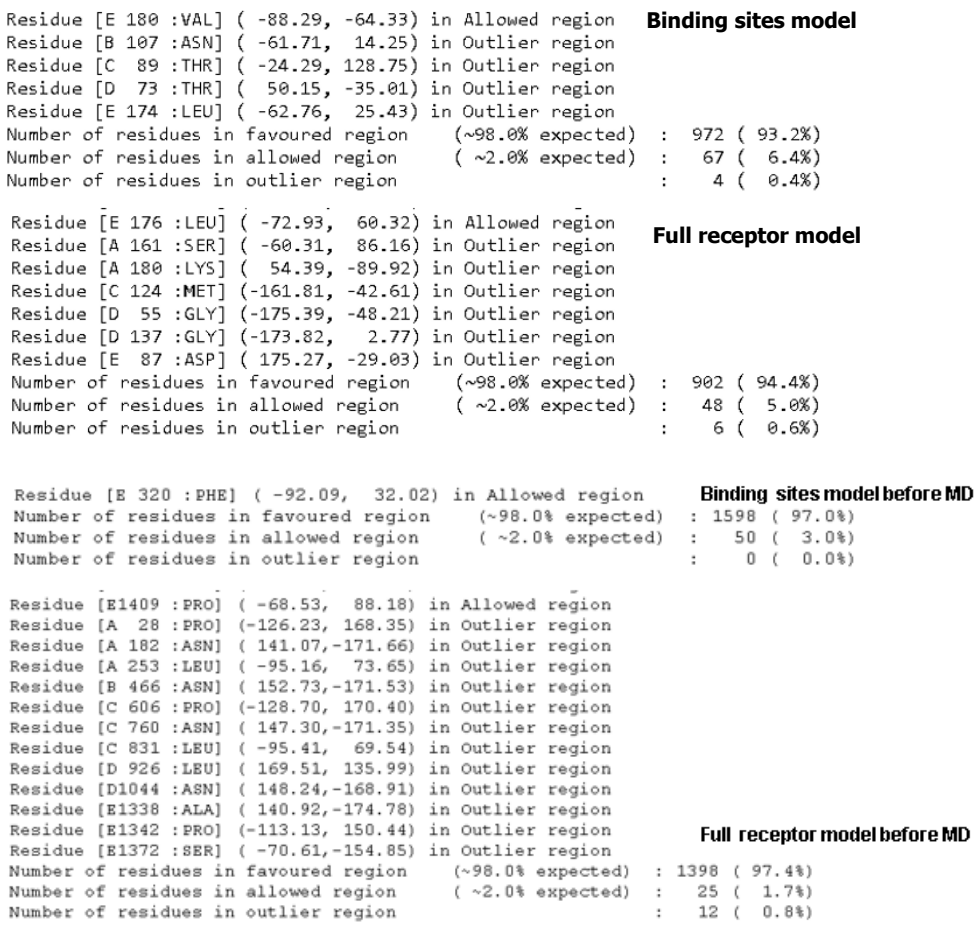

Figure 8. Ramachandran plot evaluation done by RAMPAGE after and prior to the MD simulations.

Analysis of the created full $GABA_AR$ model indicated that there may be an issue regarding the stability of the structure. The radius of gyration describes how compact a protein is and the results of MD simulation suggest that there was an increase in the radius of gyration value for the created full receptor model (Figure 9).

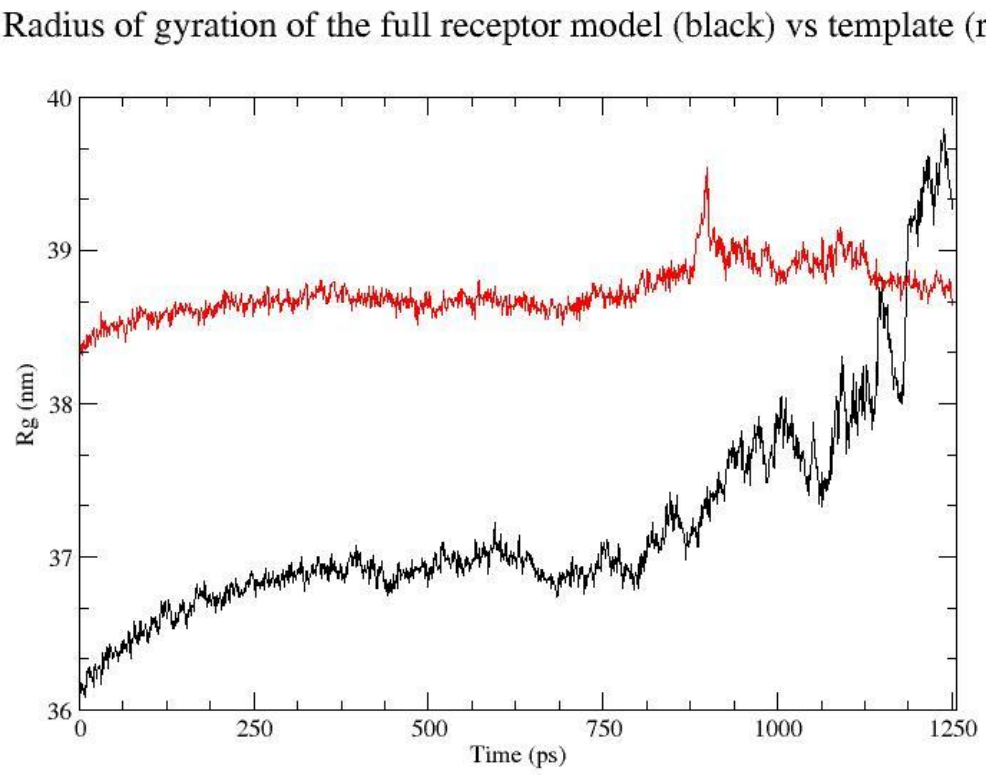

Figure 9. Radius of gyration of the full $GABA_AR$ model compared to the template (PDB ID: 4COF).

2.3. Docking

Docking was performed with no constraints and the best docking poses were selected based on the estimated free energy of binding (Prime/MMGBSA), Glide XP docking score, Induced Fit g-score and visual assessment. The best poses for the ligands were considered to be those that included most of the reported favorable interactions for the flavonoids (Renard et al., 1999; Huang et al., 2001). Such interactions include the presence of π-π stacking, salt bridges, hydrogen bonds and π-cation interactions between prenylflavonoids and the binding pocket residues. Flumazenil, bicuculline and CGS-9885 were used as reference structures in terms of the Prime/MMGBSA energies and the docking scores in their respective binding pockets.

Results obtained from docking at the potential binding sites are shown in Tables 1, 5, 7 and 8. The residues that are most likely to form strong interactions with the studied ligands are displayed in Tables 2, 3, 4 and 6.

2.4. Docking performed in the $\alpha_1\beta_2\gamma_2$ receptor isoform

The most favorable free energy of binding was predicted for 6PN in the α_1+/γ_2- andα_1+/β_2- pockets, while XN seemed to fit better than the other compounds in the γ_2-/β_2+ pocket (Table 1). 8PN had the least favorable calculated MMGBSA values in all the three putative pockets that were investigated in this structure. MMGBSA of flumazenil in its experimental binding site, prior to induced fit docking was -62.218.

Table1. Docking scores and estimated binding free energies in different binding pockets of the crystal structure of $GABA_AR$ $\alpha_1\beta_2\gamma_2$ subtype (PDB ID: 6D6U).

Binding site	**α_1+/γ_2-**	
Ligand	**Prime MMGBSA ΔGbind (kcal/mol)**	**XP g-score**
6-prenylnaringenin	-71.13	-8.255
8-prenylnaringenin	-50.65	-9.824
Xanthohumol	-45.33	-6.139
Isoxanthohumol	-63.00	-8.898
Flumazenil	-64.94	-6.882
Binding site	**α_1+/β_2-**	
Ligand	**Prime MMGBSA ΔGbind (kcal/mol)**	**XP g-score**
6-prenylnaringenin	-67.11	-8.255
8-prenylnaringenin	-60.74	-9.824
Xanthohumol	-61.74	-6.139
Isoxanthohumol	-60.97	-8.898
CGS-9895	-69.64	-6.882
Binding site	**γ_2+/β_2-**	

Ligand	Prime MMGBSA ΔGbind (kcal/mol)	Induced fit docking g-score
6-prenylnaringenin	-50.65	-6.013
8-prenylnaringenin	-50.58	-6.278
Xanthohumol	-66.97	-10.146
Isoxanthohumol	-64.54	-7.655

Hydrogen bonds involved in receptor-ligand interactions at the α_1+/γ_2- and α_1+/β_2- pockets in this structure were most commonly formed with histidine, serine and threonine, while tyrosine and phenylalanine seemed to be mostly involved in the π-π stacking interactions. At the γ_2+/β_2- putative binding pocket asparagine was mostly the residue participating hydrogen bonds (Tables 2, 3 and 4).

Table 2. Residues interacting with the docked compounds at the $\alpha_1\gamma_2$ binding pocket of $\alpha_1\beta_2\gamma_2$ $GABA_AR$ subtype

Compound	Subunit α_1	Subunit γ_2
6-prenylnaringenin	**His_{102}**, **Ser_{159}**, Ser_{205}, Ser_{206}, Tyr_{160}, **Tyr_{210}**	**Thr_{142}**, Glu_{189}
Xanthohumol	**His_{102}**, **Ser_{159}**, **Thr_{207}**	Asp_{56}, **Thr_{142}**
Isoxanthohumol	**His_{102}**, **Ser_{159}**, Tyr_{160}, **Tyr_{210}**	**Thr_{142}**
8-prenylnaringenin	Ala_{101}, **His_{102}**, **Ser_{159}**, Phe_{100}, **Tyr_{210}**	Met_{57}, Tyr_{58}
Flumazenil	Ala_{161}, **Thr_{207}**, **Tyr_{210}**	**Thr_{142}**

The residues that are predicted to form strong interactions, such as hydrogen bonds, hydrophobic interaction/van der Waals interactions or π–π stacking, with prenylflavonoids in the binding site between α_1 and γ_2 subunits at the $\alpha_1\beta_2\gamma_2$ receptor

subtype, were tyrosine 210, histidine 102, serine 159 and threonine 207 (α_1 subunit) and threonine 142 (γ_2 subunit) and they are presented in bold.

Table 3. Residues interacting with the docked compounds at the$\alpha_1\beta_2$ binding pocket of $\alpha_1\beta_2\gamma_2$ $GABA_AR$ subtype

Compound	Subunit α_1	Subunit β_2
6-prenylnaringenin	Gln_{204}, **His_{102}**, **Phe_{100}**, Ser_{159}, Ser_{205}, Ser_{206}, Tyr_{160}, **Tyr_{210}**	**Tyr_{62}**
8-prenylnaringenin	**His_{102}, Lys_{156}, Phe_{100}, Tyr_{210}**	**Tyr_{62}**
Xanthohumol	**His_{102}, Lys_{156}, Tyr_{210}**	Ala_{45}, **Tyr_{62}**
Isoxanthohumol	**His_{102}, Phe_{100}, Tyr_{210}**	**Tyr_{62}**
CGS-9895	**His_{102}**, Ser_{206}	**Tyr_{62}**

The residues that are predicted to form strong interactions with prenylflavonoids in the binding site between α_1 and β_2 subunits at the $\alpha_1\beta_2\gamma_2$ receptor subtype, were tyrosine 210, histidine 102, lysine 156 and phenylalanine 100 (α_1 subunit) and tyrosine 62 (β_2 subunit).

Table 4. Residues interacting with the docked compounds at the$\beta_2\gamma_2$ binding pocket of $\alpha_1\beta_2\gamma_2$ $GABA_AR$ subtype

Compound	Subunit β_2	Subunit γ_2
6-prenylnaringenin	**Asp_{43}**, Lys_{180}, **Tyr_{62}**	Asn_{115}
8-prenylnaringenin	Thr_{176}	Ser_{171}, Tyr_{172}
Xanthohumol	**Asp_{43}**, Ile_{44}, **Tyr_{62}**	Arg_{114}, Thr_{215}, Ser_{217}
Isoxanthohumol	**Asp_{43}**	Glu_{168}

The residues that are predicted to form strong interactions with prenylflavonoids in the binding site between β_2 and γ_2 subunits at the $\alpha_1\beta_2\gamma_2$ receptor subtype, were asparagine 43, tyrosine 62 (β_2 subunit). It was not possible to determine what residues from the γ_2 subunit would make strong interactions at this interface.

2.5. Docking results from the $\alpha_1\beta_3\gamma_2$ crystal structure

Results from the docking studies at the $\alpha_1\beta_3\gamma_2$ isoform crystal were somewhat different at the two $\alpha\beta$ interfaces. From all the hops compounds, IXN had the highest values at the interface of A and B chains interface, whereas 8PN seemed to have the best scores at the interface of D and E chains. 6-prenylnaringenin had the least desirable docking results in both studied pockets (Table 5). Bicuculline had the best scores in both pockets. Residues that were most reoccurring in the formation of interactions with the hops compounds at these sites are shown in Table 6.

Table 5. Docking scores and estimated binding free energies in different binding pockets of the crystal structure of $GABA_AR$ $\alpha_1\beta_3\gamma_2$ subtype (PDB ID: 6HUK).

Binding site	**α_1+/β_3− (AB chains)**	
Ligand	**Prime MMGBSA ΔGbind (kcal/mol)**	**XP g-score**
6-prenylnaringenin	-46.36	-8.412
8-prenylnaringenin	-49.76	-8.486
Xanthohumol	-47.75	-6.807
Isoxanthohumol	-54.65	-8.727
Bicuculline	-66.33	-10.072
Binding site	**α_1+/β_3− (DE chains)**	
Ligand	**Prime MMGBSA ΔGbind (kcal/mol)**	**XP g-score**
6-prenylnaringenin	-32.57	-6.751
8-prenylnaringenin	-36.47	-6.906

Xanthohumol	-36.28	-5.852
Isoxanthohumol	-36.21	-6.767
Bicuculline	-53.74	-9.317

Table 6. Residues interacting with the docked compounds at the$\alpha_1\beta_3$ binding pocket of $\alpha_1\beta_3\gamma_2$ $GABA_AR$ subtype

Compound	Subunit α_1	Subunit β_3
6-prenylnaringenin	Phe156	**Glu155, Tyr157**
8-prenylnaringenin	**Phe46**	Arg207, **Glu155, Tyr157**
Xanthohumol	Arg173, Asp44, **Phe46**	**Glu155, Tyr157**
Isoxanthohumol	Arg207, **Phe46**, Tyr157	**Glu155, Tyr157**
Bicuculline	**Phe46**, Phe65	**Glu155,** Phe200, **Tyr157,**

The residues that are predicted to form strong interactions with prenylflavonoids in the binding site between α_1 and β_3 subunits at the $\alpha_1\beta_3\gamma_2$ receptor subtype, were phenylalanine 46 (α_1 subunit) and glutamine 155 and tyrosine 157 (β_3 subunit).

2.6. The binding sites receptor model and the full receptor model of $\alpha_6\beta_3\delta$ $GABA_AR$ subtype

The docking results for the binding sites receptor indicate that XN may have the highest affinity towards $\alpha_6\delta$ and $\beta_3\delta$ interfaces. 8PN seemed to have the least favorable scoring at the $\alpha_6\beta_3$ and $\beta_3\delta$ sites, while the docking scores ranked 6PN the best at the $\alpha_6\beta_3$pocket and the lowest at the $\alpha_6\delta$ binding site (Table 7).

Table 7. Docking scores and estimated binding free energies in different binding pockets of the binding sites receptor model ($\alpha_6\beta_3\delta$).

Binding site	α_6+/δ–	
Ligand	**Prime MMGBSA ΔGbind (kcal/mol)**	**Induced fit docking g-score**

6-prenylnaringenin	-35.18	-4.291
8-prenylnaringenin	-37.94	-4.500
Xanthohumol	-62.16	-6.787
Isoxanthohumol	-44.98	-5.234
Binding site	α_6+/β_3-	
Ligand	**Prime MMGBSA ΔGbind (kcal/mol)**	**Induced fit docking g-score**
6-prenylnaringenin	-58.79	-8.826
8-prenylnaringenin	-42.56	-4.122
Xanthohumol	-51.83	-6.120
Isoxanthohumol	-49.32	-4.207
Binding site	$\beta_3-/\delta+$	
Ligand	**Prime MMGBSA ΔGbind (kcal/mol)**	**Induced fit docking g-score**
6-prenylnaringenin	-59.97	-8.264
8-prenylnaringenin	-52.50	-7.577
Xanthohumol	-72.15	-9.391
Isoxanthohumol	-59.71	-7.782

The full receptor model results were significantly inferior compared to those of the binding sites model. The only compound that had the same ranking at the binding pockets was 8PN, however scoring was notably different. Best docking values were obtained at $\alpha_6\delta$, $\alpha_6\beta_3$ and $\beta_3\delta$ for 6PN, XN and IXN, respectively. XN seemed to have the lowest affinity at the $\alpha_6\delta$ binding site (Table 8).

Table 8. Docking scores and estimated binding free energies in different binding pockets of the full receptor model ($\alpha_6\beta_3\delta$).

Binding site	α6+/δ–	
Ligand	**Prime MMGBSA ΔGbind (kcal/mol)**	**Induced fit docking g-score**
6-prenylnaringenin	-35.18	-4.291
8-prenylnaringenin	-40.13	-4.949
Xanthohumol	-30.86	-4.747
Isoxanthohumol	-39.95	-5.452
Binding site	α6+/β3–	
Ligand	**Prime MMGBSA ΔGbind (kcal/mol)**	**Induced fit docking g-score**
6-prenylnaringenin	-44.95	-4.895
8-prenylnaringenin	-35.06	-5.602
Xanthohumol	-50.94	-6.779
Isoxanthohumol	-40.37	-4.850
Binding site	β3–/δ+	
Ligand	**Prime MMGBSA ΔGbind (kcal/mol)**	**Induced fit docking g-score**
6-prenylnaringenin	-55.73	-6.510
8-prenylnaringenin	-41.27	-6.306
Xanthohumol	-46.42	-5.846
Isoxanthohumol	-55.11	-6.675

The values from the full receptor model and the binding sites model were notably lower compared to the values in the crystal structures and are considered unreliable. Due to this the interacting residues in the studied binding pockets of these two structures were not analyzed.

3. Discussion

3.1. Flumazenil/BZD binding site (α1γ2)

Experimental data has shown that the modulatory action of prenylated flavonoids is flumazenil insensitive (Hall et al., 2004; Benkherouf et al., 2019). Hence, the good docking scores (comparable or slightly better than those of flumazenil) of hops compounds were unexpected. Nonetheless, there is some evidence that flavonoids could act the flumazenil-sensitive sire as well (Johnston et al., 2015). It should be kept in mind that the docking is done by an algorithm that optimizes the ligand interactions with the receptor and cannot be fully relied on. Furthermore, prenylated flavonoids were shown to act as allosteric modulators (Benkherouf et al., 2019) on $GABA_AR$, which means that the presence of the neurotransmitter GABA is required for the hops exert their action on the receptor. For simplicity's sake, all docking studies were carried out on a receptor structure/model that did not have GABA present, as its presence would make MD simulations longer and more complex. Only the $\alpha_1\beta_2\gamma_2$ and $\alpha_1\beta_3\gamma_2$ $GABA_AR$ crystals (6D6U, 6HUK, respectively) contain GABA but it was removed before docking.

Based on receptor-based pharmacophore models it may be possible to explain the good scores of the hops compounds at the flumazenil/BZD binding site. Richter et al., 2012, and Bergman et al., 2013, reported several residues as important for interacting with ligands at the BZD site. For example, His101 (His102 in our study) in the α_1 subunit as a positively charged amino acid and Phe99 (Phe100) and Tyr159 (Tyr160) that also are part of this subunit as hydrophobic interaction points were proposed to be involved in interacting with ligands. In γ_2 subunit, Phe77 was reported as important hydrophobic determinant for the binding of ligands. These residues are also noted as important ligand-interacting amino acids in this modeling study. These residues are likely to be involved in flavonoid binding, as some of the flavonoids' effects are thought to be a result of interacting with the BZD binding site (de Oliveira et al., 2018). For ligands to bind at the benzodiazepine site it is necessary that they possess at least two hydrogen bond donating moieties and one moiety that would accept a hydrogen bond. The ligands should also be positioned in such a manner that they are able to have lipophilic interactions with a certain region of the binding pocket (Clayton et al., 2007).

A 3D-QSAR flavonoid pharmacophore model proposed by Huang et al., 2001 identified features on 6PN that contribute to its good binding at the αγ site. 6PN carbon atoms at

position 6 and 7 (and their substituents) (Figure 10) were shown to be high sensitivity sites regarding the affinity towards the BZD site of the receptor. Moreover, the 3D-QSAR pharmacophore model proposes two hydrogen bond acceptors, and two hydrophobic sites of interaction, which can be observed in our study in the obtained 6PN interaction with the $\alpha_1\gamma_2$binding pocket. Additionally, the conformation of 6PN in our study corresponds to those predicted from 38 structures as a possible binding conformation, in the same 3D-QSARstudy done by Huang et al., 2001 (Figure 11). It should be noted that their unified pharmacophore model did not account for flavanones, which differ in structure from flavones as there is no double bond present between the carbon atoms C2 and C3. This double bond is assumed to be important for the planarity of the structures and binding to the classical BZD site although there are still discrepancies with regard to the structure for the pharmacophore model of flavonoids (Dekermendjian et al., 1999; Hall et al., 2005).

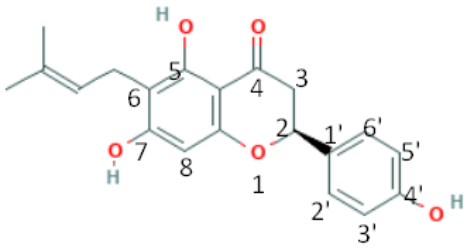

Figure 10. Numbering of the carbon atoms in 6-prenylnaringenin and other prenylflavonoids. Hydroxyl group is present at position 7 and prenyl group at position 6.

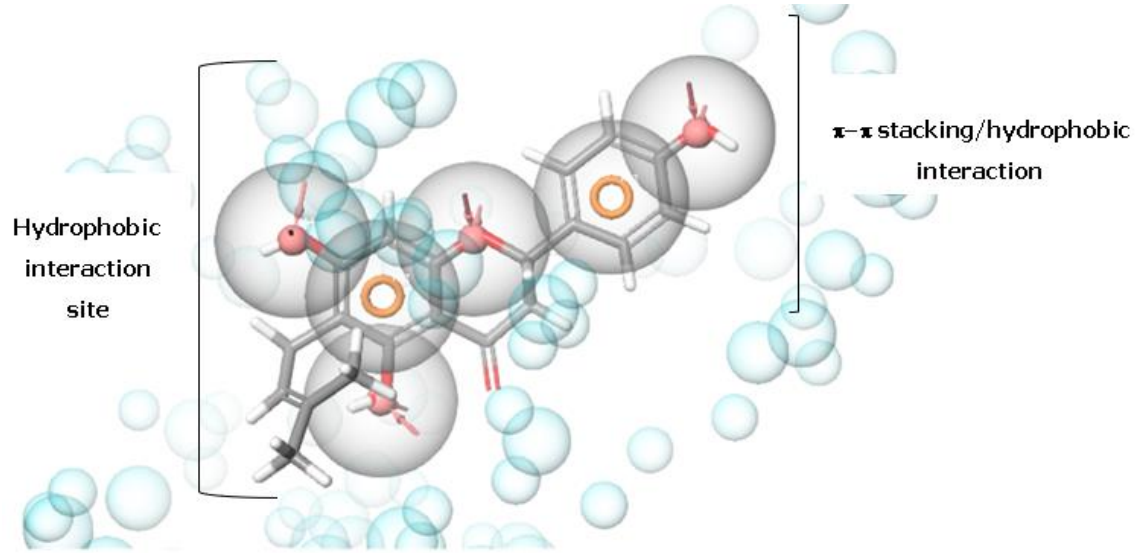

Figure 11. Huang et al.'s (2001) pharmacophore hypothesis model of 6PN in $\alpha_1\gamma_2$ binding pocket of $GABA_AR$ regenerated by us with the Phase tool in Maestro. Carbon atoms of 6PN are colored grey, hydrogen atoms are displayed in white and oxygen atoms are shown in red. The red arrows point out the acceptor atoms, and orange rings are placed at the aromatic ring centers of 6PN. The two hydrophobic groups proposed by Huang et al's 3D-QSAR model are marked with the black lines.

Compared to other hops compounds studied in this project 6PN is the only one with a substituent at position 6. This site was speculated to be the one where either hydrogen bond or electrostatic interactions occur between ligands and the binding site residues (Huang et al., 2001). Figure 12 shows the 2D interactions between the residues located in the $\alpha_1\gamma_2$pocket and the docked 6PN.

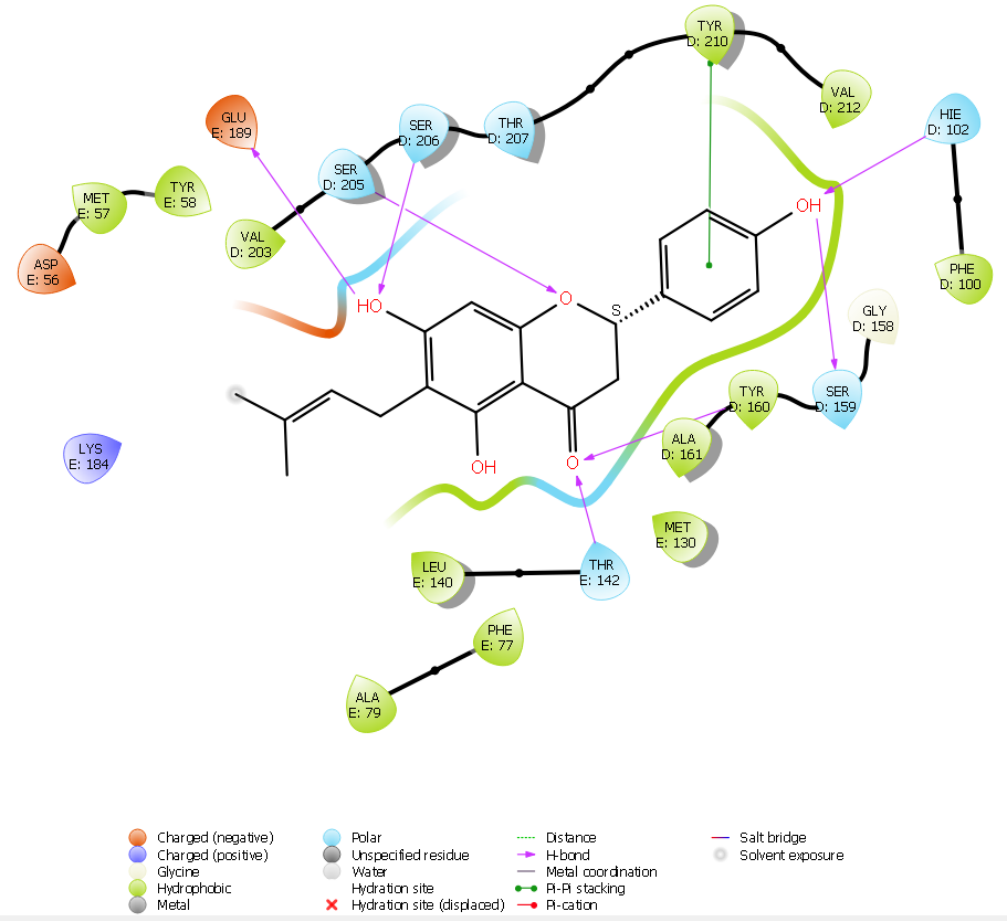

Figure 12. 2D representation of the ligand-receptor interactions of the docked 6PN at the $\alpha_1\gamma_2$ pocket in $GABA_AR$. The conformation of both receptor and ligand enables for the high amount of hydrogen bonds (purple arrows) and a $\pi-\pi$ stacking interaction between the phenyl ring of 6PN and Tyr210 of the α_1 subunit.

The residues that interact with the studied compounds are consistent with those obtained from the experimental data to be important for binding of agonists at the $\alpha_1\gamma_2$ pocket of $GABA_AR$; tyrosine 210, threonine 142 (of α_1 subunit) and phenylalanine 77of γ_2 subunit (Buhr et al., 1996; Jursky et al., 2000) Furthermore, a β–rich domain in the extracellular domain of $GABA_AR$ was described in the progressive deletion experiments (Xue et al., 1999, 2000). Some of the most significant ligand binding residues belong to this domain, such as tyrosine 161 (Tyr160 in our study), threonine 162, glycine 200 and threonine 206 (Thr207 in our study), and they are part of the α_1 subunit. The docked 6PN at the $\alpha_1\gamma_2$ pocket interacts closely with some of those residues (Figure 13).

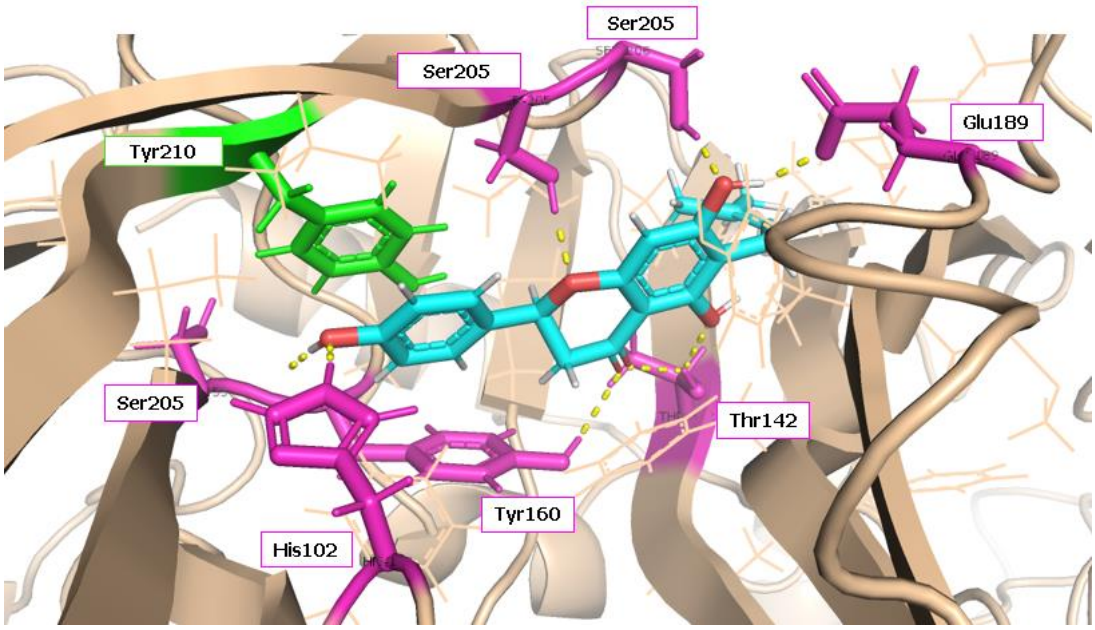

Figure 13. 6-prenylnaringenin interactions at the α_1/γ_2 binding site of the $GABA_A$ receptor isoform $\alpha_1\beta_2\gamma_2$ (PDB ID: 6D6U; light pink, cartoon and lines representation). Carbon atoms of 6-prenylnaringenin are colored in cyan, oxygen atoms in red and hydrogen atoms in white. Residues that form hydrogen bonds with 6-prenylnaringenin are colored in magenta and π-π stacking residues are colored in green. The most important interactions are π-π stacking interactions between the aromatic ring of 6-prenylnaringenin and tyrosine 210 and polar (hydrogen bonding) interactions of 6-prenylnaringenin with threonine 142, glutamine 189, histidine 102, serine 159, serine 205 and serine 206. Polar interactions are shown as dotted yellow lines.

3.2. The CGS-9895 binding site binding pocket between α_1+/ β_2-subunits

According to the docking results for the binding pocket between the α_1+ and β_2– subunits, 6PN seems to fit best into this pocket. However, all of the prenylflavonoids had comparable scores at this pocket. The reference compound CGS-9895, which acts as a positive allosteric modulator at the αβ site (Varagic et al., 2013) exhibited the highest MMGBSA binding energy. Point mutations at the α1 subunit have indicated that tyrosine 209 (Tyr210 in our study) was the key residue involved in the mode of action of CGS-9895 (Maldifassi et al., 2016; Ramerstorfer et al., 2011). Even though tyrosine 210 did not form interactions such as hydrogen bonds or π–π stacking with CGS-9895 in our docking model, it was a part of the hydrophobic pocket in the binding site (Figure 14).

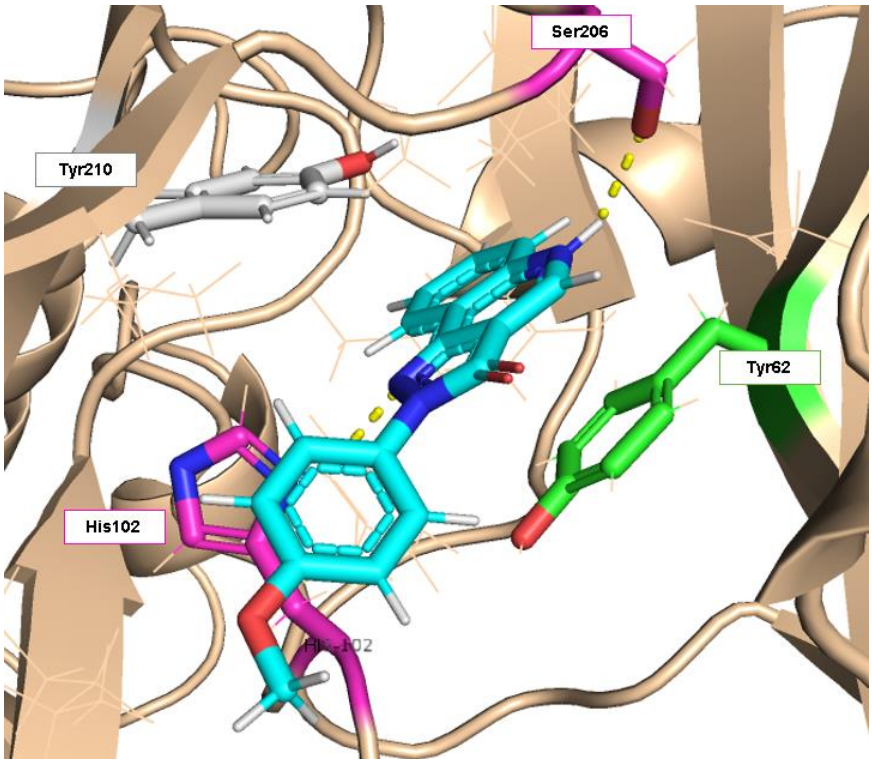

Figure 14. CGS-9895 interactions at the α_1/β_2 binding site of the $GABA_A$ receptor isoform $\alpha_1\beta_2\gamma_2$ (PDB ID: 6D6U; light pink, cartoon and lines representation). Carbon atoms of CGS-9895 are colored in cyan, oxygen atoms in red, nitrogen atoms in blue and hydrogen atoms in white. Carbon atoms of residues that form hydrogen bonds with CGS-9895 are colored in magenta and carbon atoms of residues involved in π-π stacking or hydrophobic interactions are colored in green and white, respectively. The most important interactions are π-π stacking interactions between the aromatic rings of CGS-9895and tyrosine 62 and

polar interactions (hydrogen bonding) with histidine 102 and serine 206. Polar interactions are shown as dotted yellow lines.

As seen in Table 3, the most important residues interacting with the docked ligands at this binding pocket were tyrosine 210, histidine 102, lysine 156 and phenylalanine 100 (α_1 subunit). As mentioned earlier, these residues are important for binding of agonists at the $GABA_AR$. Figure 15 shows 8PN interactions in this binding pocket.

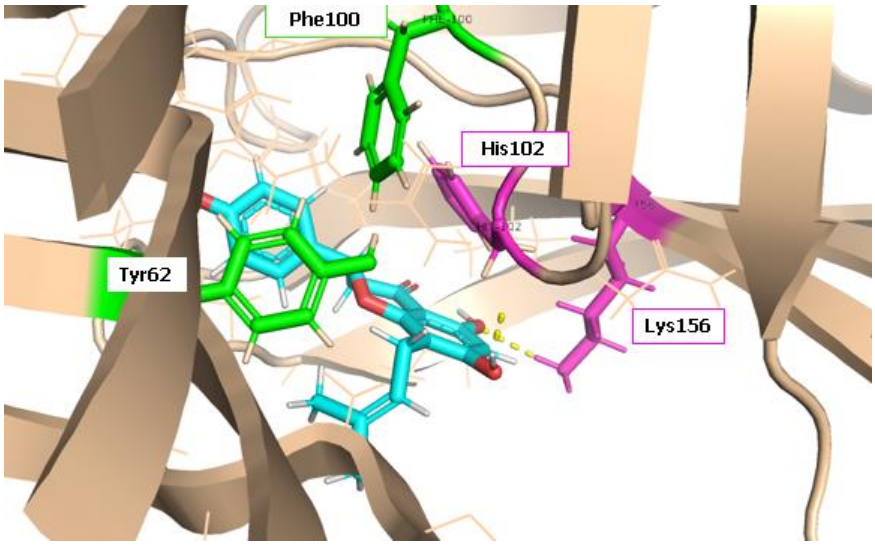

Figure 15. 8-prenylnaringenin interactions at the α_1/β_2 binding site of the $GABA_A$ receptor isoform $\alpha_1\beta_2\gamma_2$ (PDB ID: 6D6U; light pink, cartoon and lines representation). Carbon atoms of 8-prenylnaringenin are colored in cyan, oxygen atoms in red and hydrogen atoms in white. Residues that form hydrogen bonds with 8-prenylnaringenin are colored in magenta and π-π stacking residues are colored in green. The most important interactions are π-π stacking interactions between the aromatic rings of 8-prenylnaringenin and phenylalanine 100 and tyrosine 62 and polar interactions (hydrogen bonding) with histidine 102 and lysine 156. Polar interactions are shown as dotted yellow lines.

Based on the docking score results this may be the most likely binding site of all studied pockets in this crystal structure, however one should keep in mind that the scoring functions can not be fully relied on.

3.3. β_2-/γ_2+binding pocket

Docking scores at the $\alpha_1\beta_2\gamma_2$ isoform seem to be the lowest at the $\beta_2\gamma_2$ subunit interface (Table 1) for 6PN and 8PN but among the best for XN and IXN. The fact that all the

tested prenylflavonoids had different interactions with residues at the γ_2 subunit may indicate that they either have different binding modes at this site or that the site is located at a different interface position. Notable at this site is the absence of the histidine 102 residue from the α_1 subunit that was experimentally determined as important for binding of benzodiazepine agonists (Wieland et al., 1992). This could mean that the histidine residue affects the binding of allosteric modulators such as prenylflavonoids and thus, they may have a preference towards interfaces that contain an α subunit.

3.4. $\alpha_1\beta_3\gamma_2$ receptor subtype

The docking scores at the crystal structure of $\alpha_1\beta_3\gamma_2$ are significantly worse than those at $\alpha_1\beta_2\gamma_2$. This may result from the fact that the docking site for $\alpha_1\beta_3\gamma_2$ structure was selected to be the pocket where bicuculline experimentally binds. This pocket is located in the extracellular domain between α_1 and β_3 subunits. However, unlike the pockets studied in the $\alpha_1\beta_2\gamma_2$ structure and the $\alpha_6\beta_3\delta$ models, orientation of α and β subunits is different. While the experimental binding site of flumazenil and the pseudo-ligand binding sites at the $\alpha_1\beta_2\gamma_2$ crystal structures are $\alpha+\beta-$, the binding sites of bicuculline are $\alpha-\beta+$. Moreover, the subunits take such conformations that the chloride channel of the receptor remains closed (Masiulis et al., 2019). This could mean that the studied prenylflavonoids have higher affinity towards the $\alpha+\beta-$ orientation of the subunits and this contributes to the assumption that the studied hops compounds act as positive allosteric modulators. Furthermore, while the aromatic residues in the $\alpha-\beta+$ pocket, such as Phe65 in α_1, Tyr157, Phe200 and Tyr205 in β_3 ($\alpha\beta$ chains) form hydrogen-bonding, $\pi-\pi$ stacking, $\pi-$cation and salt bridge interactions with the isoquinoline and phthalide rings of bicuculline, these interactions are not established between the pocket residues and the hops compounds. For example, Phe200 in β_3 is not in favorable orientation to be able to interact with IXN. Aromatic ring of the amino acid seems to be too far (more than 4.4 Å, which is considered to be optimal for establishing $\pi-\pi$ stacking) from any of the rings of IXN. Additionally, the position of the phenylalanine aromatic ring is oriented so that it cannot interact with the IXN rings (Figure 16).

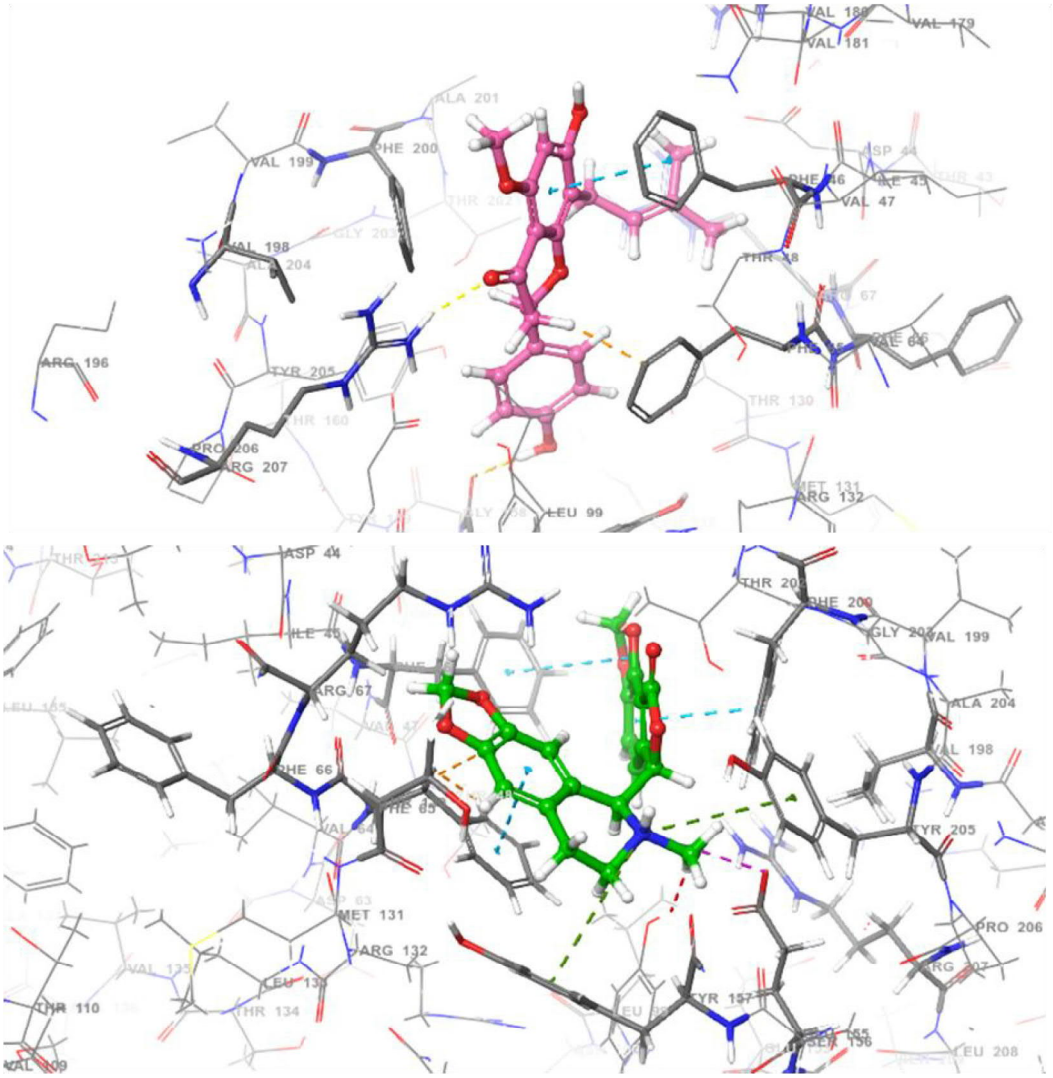

Figure 16. Predicted binding mode of IXN (top) and experimental binding mode of bicuculline (bottom) in the $\alpha_1\beta_3$ binding site of the $\alpha_1\beta_3\gamma_2$ isoform crystal structure (A and B chains; PDB ID 6HUK), respectively. Carbon atoms of IXN and bicuculline are colored in magenta and green, respectively. All oxygen atoms are colored in red, nitrogen atoms in blue, and all hydrogens are colored in white. The binding site residues have carbon atoms colored grey. π–π and π–cation interactions are presented as blue and green dashed lines, respectively. Hydrogen bond interactions are shown as yellow dashed lines.

Interestingly, the docking results for the two identical $\alpha_1\beta_3$ binding sites (between chains A and B or D and E) are somewhat different, A/B interface resulting into better docking scores than the D/E interface. Bicuculline scores were clearly better than those of the prenylflavonoids. However, the scores differed somewhat in the two binding sites for bicuculline as well.

For example, between chains A and B the best scoring (although not very high in any case) of hops compounds was calculated for IXN. In contrast, at the D/E interface the free energy of binding for IXN was significantly worse. Superimposing the A/B and D/E binding sites may explain the differences between the docking scores at these identical sites. In the less favorable (D/E) pocket the conformation of the ligand-receptor complex has lower number of interacting residues with IXN and greater number of steric clashes. For example, in the A/B binding pocket IXN has π–π stacking interactions with Phe46 and Tyr147 and hydrogen bond interactions with Arg207. The D/E interface showed only hydrogen bond interactions between IXN and Glu155. In fact, IXN has a different pose in both sites (Figure 17). In contrast, bicuculline seems to have quite similar poses in both pockets, and there are no significant differences between the binding pocket residues' positions. However, minute differences in the binding site conformation likely cause the somewhat different binding scores.

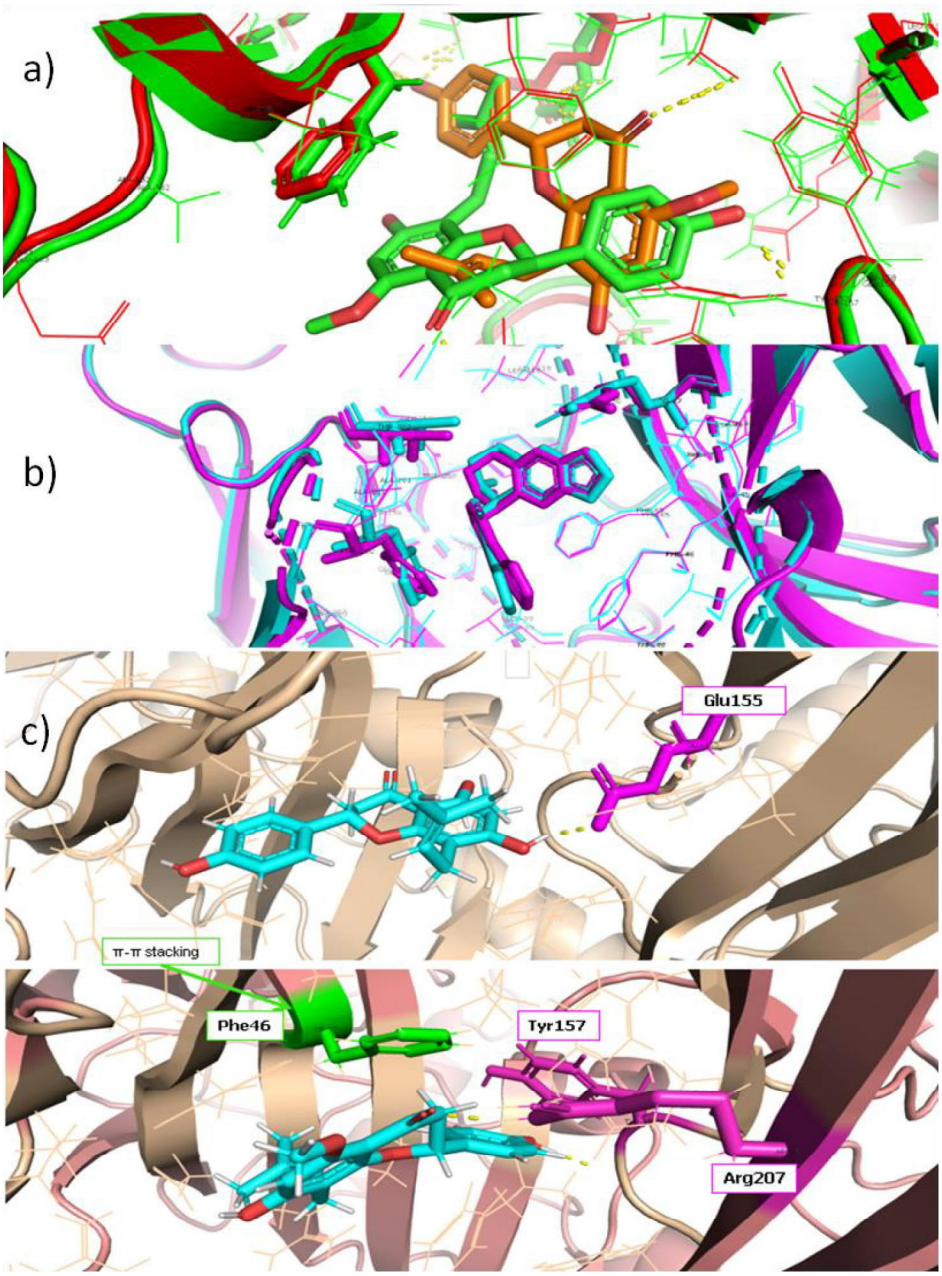

Figure 17. a) IXN pose at the α1β3 binding pocket between A and B protein chains versus between D and E chains at the $\alpha_1\beta_3\gamma_2$ $GABA_AR$ subtype (PDB ID: 6HUK). A/B site residues are colored in green, D/E site residues are colored in red. IXN bound at the A/B interface has carbon atoms colored green and IXN at the D/E pocket has carbon atoms colored orange; b) bicuculline in A/B (blue) and D/E (purple) binding pockets of the $GABA_AR$; c) interactions of IXN with the side chain residues in the D/E (top) and AB (bottom) interface. Carbon atoms of IXN are colored cyan, all oxygen atoms are colored red and all hydrogens are colored white. Hydrogen bond interactions are shown as yellow dashed lines.

8PN had clearly lower values than bicuculline, although it was among the top ranked compared to other hops compounds (Table 5). Low docking score values for the prenylflavonoids may also be resulting from the conformation of the receptor taken after bicuculline binding. Bicuculline binding induced the change in conformation of the subunits (Masiulis et al., 2019) and this may be unfavorable for the binding of prenylflavonoids.

Despite the poor scoring, 8PN can fit well into the pocket since it has the two hydrogen donors, one hydrogen acceptor and a notable hydrophobic interaction site, and these features were proposed to be required for flavonoids to bind successfully at $GABA_AR$ (Huang et al., 2001; Clayton et al., 2007). This is presented in Figure 18.

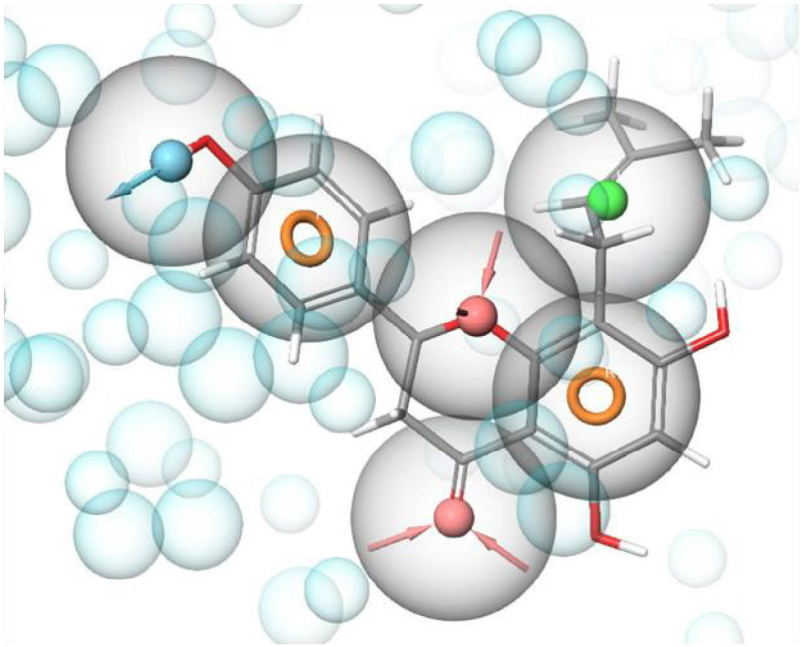

Figure 18. Simplified pharmacophore hypothesis model of 8PN in $\alpha_1\beta_3$ binding pocket of $GABA_AR$ (PDB ID: 6HUK) done by Phase in Maestro, based on Clayton et al.'s (2007) work. Carbon atoms of 8PN are colored grey, hydrogen atoms are displayed in white and oxygen atoms are shown in red. The red arrows point out acceptor atoms, and orange rings are placed at the aromatic ring centers of 8PN. Blue arrow represents hydrogen donor and the green sphere shows a hydrophobic site.

3.5. Receptor models of the α6β3δ isoform

In general, docking scores in the $\alpha_6\beta_3\delta$ binding sites model and especially the full receptor model are significantly worse than those in the crystal structures of the other two isoforms (Tables 1, 7, 8). Nonetheless, the best calculated Prime/MMGBSA binding energy of a prenylflavonoid was obtained at this receptor subtype. Despite the fact that both the models represent the same binding sites, the docking score/binding energy values for the same compounds in the same representative sites in these models were different. Most notable was XN scoring at the α_6/δ site; in the binding sites model it had the best values, whereas in the full receptor model it was scored as the worst. This can be explained by the differences in positions of the residues that form the pocket. There are less steric clashes and more favorable interactions between XN and the amino acids at the binding sites receptor model (Figure 19).

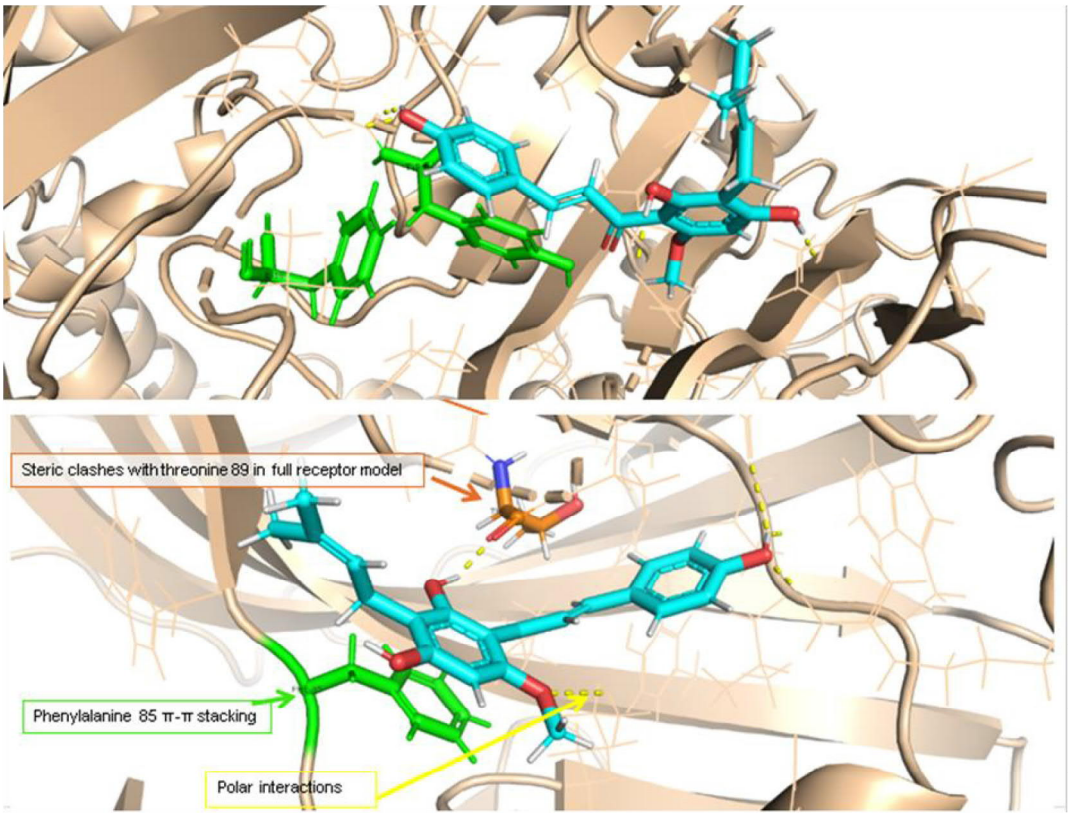

Figure 19. XN interactions at the α_6/β_3 binding sites of the $\alpha_6\delta_3\delta$ $GABA_A$ receptor isoform in the binding sites model (top) and full receptor model (bottom). Carbon atoms of XN are colored in cyan, all oxygen atoms are colored in red, nitrogen atoms in blue and all hydrogen atoms in white. Residues that form π-π stacking interactions with XN are colored in green. Threonine that causes a steric clash with XN has carbon atoms colored in orange. Polar interactions are shown as dotted yellow lines.

Experimental data has indicated that out of the studied hops compounds 8PN has the highest affinity towards the $\alpha_6\beta_3\delta$ $GABA_AR$ subtype (Benkherouf et al., 2019). 8PN had the worst docking score/binding energy values in two out of the three tested binding pockets. However, based on the docking scores/binding energies (Table 8), the most likely binding site for 8PN and the other prenylflavonoids at this receptor subtype could be the $\beta_3\delta$ site. Contrary to the experimental data that has shown XN to exhibit the lowest binding affinity to $GABA_AR$ of the prenylflavonoids (tested on $\alpha_1\beta_3\gamma_2$, $\alpha_2\beta_3\gamma_2$ and $\alpha_6\beta_3\delta$ subtypes, expressed in HEK293 cell line) (Benkherouf et al., 2019), in this project it seemed to show the highest affinity towards most of the binding sites where the hops compounds were docked.

Even though the docking scores/binding energy estimates suggest $\beta_3\delta$ as the most likely binding site for prenylflavonoids at the $\alpha_6\beta_3\delta$ $GABA_AR$ subtype, other sites may be possible too, if the conformation of the side chains would be different. Without an experimental structure of the $\alpha_6\beta_3\delta$ $GABA_AR$ subtype, it is not possible to know exactly what the ligand-binding conformation of the residues at the receptor binding sites is. The inaccurate conformation is likely the reason why the scores are so low, especially in the case of the full receptor model.

Another important note is that with the used methods and models it is difficult to give any definite ligand-receptor affinities as the scoring algorithms are inaccurate and depend largely on the binding site conformation (Chen, 2015; Li et al., 2019). Some of the scoring functions work well for specific targets but could be incorrect for the others and docking poses can be scored well, despite not being the correct ones (Scior et al., 2012; Bauer et al., 2013).

Moreover, if any of the residues in the full receptor model used in this study was misaligned, it may have led to a wrong binding site model or misplacement of other structurally crucial residues, which then affects the stability of the protein (during the MD simulation). This can occur when incorrect alignment causes the orientation or solvent accessibility of the residues that make up the active sites to take a false conformation (Burke et al., 1999) Even though the models used here were energy minimized and equilibrated, such steps do not lead to recovering from alignment errors (Marti-Renom et al., 2000).

In summary, the obtained results suggest that prenylflavonoids may bind to more than one pocket in the extracellular domain of the studied $GABA_AR$ subtypes. It was not possible to definitely distinguish high affinity binding sites from low affinity binding sites as the docking results varied for each compound in the studied pockets. Furthermore, even the same subunits' interface pockets on the different $GABA_AR$ subtypes could be different for the same compounds (due to different binding site conformations) as it was the case for the full receptor model and the binding sites model of the $\alpha_6\beta_3\delta$ $GABA_AR$ subtype. Molecular modeling approaches can aid in predicting unknown binding sites of compounds at their target proteins. However, there are limitations such as inaccurate scoring functions and lack in the accuracy of modelling the binding sites. The possible occurrence of inadequate and false results may be partly omitted by the use of more exhaustive methods such as MD simulations. These methods take into the account the flexibility of the receptor. However, in order to determine the binding site and binding mode of the prenylated flavonoids most accurately, experimental structure determination by X-ray crystallography could be attempted.

Based on the literature and the data obtained from this project, there are some propositions for future studies. For example, a ligand-binding assay that would include CGS-9895 could be attempted with the aim to determine if its activity is blocked by the hops compounds. As previously discussed, the interface in the ECD of $GABA_AR$ that is assembled from the $\alpha+/\beta-$ subunit is positively allosterically modulated by this pyrazoloquinoline. This suggests that if hops compounds block or reduce the effects on the $GABA_AR$ that resulted from this compound, the pocket in which they bind may be the same. Furthermore, ligand-binding assays that would include flurazepam might be useful as well, since this compound was reported to share the same site of action as CGS-9895 (ref). However, there are some conflicting experimental data whether the site of action is shared between these two compounds (Maldifassi et al., 2016, Ramerstorfer et al. 2011). Flurazepam has likely multiple sites of action and recently it was shown to act through the $\alpha_1\gamma_2$ site of the $\alpha_1\beta_2\gamma_2$ $GABA_AR$ subtype (Jatczak-Śliwa et al., 2018). The docking study performed in this project showed this site to be potentially interacting with the prenylflavonoids. Thus, assays with flurazepam may yield new insight into the location of the exact binding pocket and the subunit preference of hops compounds.

4. Required Methodology, Materials and Methods including Experimental Design

4.1. Protein and ligand structure preparation.

Protein Data Bank ([PDB]; available at: www.rcsb.org; Berman et al., 2000) was used to study the available $GABA_AR$ structures complexed with various ligands. The $GABA_AR$ $\alpha_1\beta_2\gamma_2$ isoform has been crystallized with the known BZD antagonist flumazenil (PDB ID 6D6U, resolution3.92 Å; Zhu et al., 2018) and $GABA_AR$ $\alpha_1\beta_3\gamma_2$isoform with the competitive $GABA_AR$ antagonist bicuculline (PDB ID 6HUK; resolution 3.69 Å; Masiulis et al., 2019).As a template for creating a model of the $\alpha_6\beta_3\delta$ isoform, a homopentameric (β_3 subunit) $GABA_AR$ was used (PDB ID 4COF; resolution 2.97 Å; Miller and Aricescu, 2014). All structures were investigated and visualized using the Maestro molecular modelling package (version 2019-1; Schrödinger, LLC) and PyMOL-visualization tool (The PyMOL Molecular Graphics System, Version 2.3 Schrödinger, LLC.).Protein crystal structures were pre-processed with the Protein Preparation Wizard of Maestro; missing hydrogens were added and water molecules were removed. All co-crystallized ligands and glycans that were not needed for the purpose of this study were removed.

Two-dimensional structures of 6PN, 8PN, IXN, XN, bicuculline, flumazenil and pyrazoloquinoline 2-p-methoxyphenylpyrazolo[4,3-c]quinolin-3(5H)-one (CGS-9895) were obtained from PubChem (Kim et al., 2019) and converted to 3D with the LigPrep tool of Maestro.CGS-9895 is experimentally determined as ligand that binds at the $\alpha+/\beta-$ pocket in the extracellular part of the receptor. Furthermore, it is shown that thetypes of the α and β subunits dictate the type of modulation by the CGS-9598 (Ramerstorfer et al., 2011). However, the clinical use of this pyrazoloquinoline is limited due to low solubility of the compound. Nevertheless, the structure, topology and the affinity that this compound has for the $GABA_AR$ make it a common template for the pharmacophore-receptor models (Huang et al., 2000).Protein structures were pre-processed with protein preparation wizard of Maestro; water molecules were removed, and missing hydrogens were added. All present ligands and glycans that were not needed for the purpose of this study were removed prior to preprocessing of the crystal structures.

4.2. Homology modeling.

The receptor subunits that were needed for the study but were not available from the PDB were created using the homology (comparative) modeling approach. The modeling alignments of the α_6 and δ subunits were generated using the multiple sequence alignment tool ClustalOmega (available at: www.clustal.org/omega; Sievers et al., 2011). Another sequence alignment web tool, EMBOSS Needle (EMBL-EBI), was used for pair wise alignments (available at: www.ebi.ac.uk/Tools/psa/emboss_needle; Madeira et al., 2019). The actual model building was performed by MODELLER version 9.20 (available at: https://salilab.org/modeller, Sali et al., 1993; Webb et al., 2016).

MODELLER creates comparative protein models by satisfying spatial restrains (Sali and Blunder, 1993; Webb and Sali, 2014). The model creation is a step-wise procedure: (i) dihedral angle and the distance restraints on the target model are obtained from the sequence alignment of the model sequence with the template 3D structure to reach the homology-derived restraints; (ii) the spatial restraints are imposed by the use of CHARMM22 force field (MacKerell et al., 1998) to obtain an objective function that is dependent on the Cartesian coordinates of the modeled molecules; (iii) the final model is created by optimizing the objective function in Cartesian space by applying the variable target function method (Braun and Go, 1985), using the conjugate gradients approach and molecular dynamics with simulated annealing (Clore et al., 1986).

Protein sequences of the $GABA_AR$ subunits α_6 and δ were obtained in FASTA format from the UniProt Knowledgebase (available at: www.uniprot.org; sequence entries Q16445 and O14764, respectively). The Protein BLAST tool (Altschul et al., 1990) was used to find similar proteins and consequently the multiple sequence alignment was created using the ClustalOmega tool. Crystal structures of $GABA_AR$ subunits (from PDB IDs: 6D6T and 6A96 and 4COF) were used as templates for the α_6 and δ subunits. Crystal structure of the homopentameric $GABA_AR$ (PDB ID: 4COF) was used as the template for the full $\alpha_6\beta_3\delta$ receptor model. Initial 10 models of each structure were created, and the quality ranking was done with the DOPE (Discrete Optimized Protein Energy) score (Shen and Sali, 2006) of MODELLER, where the lower energy value means a better model.

Additionally, a simplified $\alpha_6\beta_3\delta$ $GABA_AR$ binding sites model was created by mutating only the binding site residues of $\alpha_1\beta_2\gamma_2$ $GABA_AR$ in the 6D6U crystal structure; mutations were done based on the pair-wise sequence alignment. Mutated residues at the α_1+/γ_2- binding site were histidine 102 to arginine (His102Arg), serine 206 to asparagine (Ser206Asn) (in α_1 subunit), aspartic acid 56 to alanine (Asp56Ala), tyrosine 58 to glutamic acid (Tyr58Glu), alanine 79 to histidine (Ala79His), threonine 142 to serine (Thr142Ser) (in γ_2 subunit). Residue numbers correspond to those of the human $\alpha_1\beta_2\gamma_2$ $GABA_AR$ sequence. The residues at the α_1+/β_2- binding pocket that were mutated were His102Arg, Ser206Asn (in α_1 subunit). The mutated residues at the β_2-/γ_2+ binding pocket were arginine 114 to valine (Arg114Val), tyrosine 220 to phenylalanine (Tyr220Phe), threonine 215 to lysine (Thr215Lys), threonine 216 to serine (Thr216Ser) and serine 217 to alanine (Ser217Ala) (in γ_2 subunit).

4.3. Molecular dynamics (MD) simulations.

MD simulations were carried out to study the conformational space at the subunit interfaces by the molecular simulation package Amber 18 (Salomon-Ferrer, Case et al. 2013). Amber's primary protein force field, the ff14SB (Maier et al., 2015), was used to perform the minimization and simulations of the proteins and the *tleap* program was used to solvate the proteins and generate the input topology and coordinates of the structures. An octahedral box was selected as the most suitable for all the MD simulations, based on the lowest number of waters present. The octahedral box that extended 10 Å around the protein. Neutralization of the simulation system for the $\alpha_6\beta_3\delta$ full receptor model was done with Na+ counter ions, whereas the system for the binding sites model was neutralized with Cl- ions. The initial minimization was carried out in 6 steps (each step 200 iterations) using two algorithms, steepest descent (for the first 10 iterations) and conjugate gradient (the last 190 iterations), so that the restraint force on the proteins was slowly reduced from 10 to 0 kcal/mol$Å^2$. Likewise, equilibration of the simulation system was performed stepwise: (i) by the use of the Langevin dynamics, the system was heated for 10 ps, starting at 10 K until it reached 300 K (frequency of collision was $\gamma=1.0ps^{-1}$), keeping the constant volume with the fixed protein and the restraint force of 5kcal/ mol$Å^2$; (ii) 20 ps heating from 10 K to 300K with the Langevin dynamics, without restraint constraints on the protein; (iii) 20 ps at constant temperature (300 K) and volume(Langevin dynamics and frequency of collision $\gamma=0.5ps^{-1}$) and with no constraints applied; (iv) 50 ps at 300K at constant pressure of 1 bar with 1 ps coupling constant and

no restraints; (v) 400 ps equilibration in the same conditions as the production simulation constant. The production simulations for the minimized and equilibrated structures were carried out for 25 ns at 300 K and at 1 bar pressure. SHAKE algorithm, which constraints all the bonds that include hydrogen (Elber et al., 2011), was used with the time step of 2 fs. The coupling constants to the pressure and temperature baths were 2 ps and 5 ps, respectively. The final structure frame after the simulation was minimized for 200 (10 steepest descent + 190 conjugate gradient) iterations with no restraints on the protein. MD trajectories were visualized with Visual Molecular Dynamics (VMD), molecular graphics program (Humphrey et al., 1996).

To avoid affecting the docking site conformations more than necessary, minimized and equilibrated structure of the $\alpha_6\beta_3\delta$ binding sites model was used for further docking studies. Ramachandran plot assessment was performed by the use of RAMPAGE (Lovell et al., 2003) to evaluate the stereo-chemical quality of the final structures of the receptor models before and after MD. Evaluation with the Ramachandran plot provides an overview of how the torsion angles in a protein are distributed and which angle regions are excluded because of steric hindrance. These torsion angles in the protein sequence are termed Phi (φ) and Psi (ψ). The former describes the protein backbone rotation around the nitrogen and the alpha carbon (Cα) bonds, whereas the latter describes the backbone rotation around Cα and C (carbonyl carbon) bond. The torsion angles belong to principal parameters that determine protein folding and the flexibility that is needed for a protein backbone to take a certain conformation (Morris et al., 1992). Moreover, in high quality experimental structures and protein models, all or most of the phi/psi angles are within the standard values depicted by the Ramachandran plot.

CPU expensive calculations such as MD and were performed at the supercomputers of CSC, the Finnish IT Center for Science.

4.4. Docking.

Docking of the hops compounds and the reference compounds flumazenil, bicuculline and CGS-9895 to the $GABA_AR$ crystal structures (PDB ID: 6D6U, 6HUK) and models was performed with the GLIDE tool of the Maestro package (Friesner et al., 2004) using the extra precision algorithm (XP). The Glide XP algorithm uses the empirical scoring function that favors lipophilic contacts in an atom-atom pair score between a protein and a ligand, hydrogen bonds within a protein-ligand complex and gives an entropic penalty depending on the amount of present rotatable bonds within the ligands. Furthermore, this

algorithm uses desolvation penalties if charged or polar groups from ligand or protein are buried. Another crucial implementation to the XP algorithm is that it recognizes specific molecular motifs that largely contribute to the increased binding affinity (Friesner et al., 2006). In addition, docking at the two suggested putative binding sites, located at the α_1+/β_2- and β_2-/γ_2+ of $\alpha1\beta2\gamma2$ $GABA_AR$ crystal structure (PDB ID: 6D6U) (Zhu et al., 2018) was carried out with the Induced Fit protocol of Maestro.

Free energy of binding for the receptor-ligand complexes was calculated with the Prime/MMGBSA (molecular mechanics–generalized Born surface area) tool of Maestro (Jacobson et al., 2002, 2004). VSGB2.1 solvation model (Li et al., 2011) was used with the OPLS3 force field (Optimized Potentials for Liquid Simulations) in order to gain the higher accuracy in the calculations of the free binding energy between the receptor and the ligands. The free energy of binding is calculated with the MMGBSA method by employing the following equations: (i)$\Delta G_{bind} = G_{complex} - G_{receptor} - G_{ligand}$; (ii) $\Delta G_{bind} = \Delta H - T\Delta S \approx \Delta E_{gas} + \Delta G_{sol} - T\Delta S$; (iii) $\Delta E_{gas} = \Delta E_{int} + \Delta E_{ELE} + \Delta E_{VDW}$; (iv) $\Delta G_{sol} = \Delta G_{GB} + \Delta G_{Surf}$. ΔG_{bind} represents the free energy of binding and is further divided into different energy types. ΔE_{int} represents the internal energy charge, however, as the trajectories for the receptor-ligand structure that belong to the protein and the ligand are the same, this energy is dismissed. ΔE_{gas} - the energy of interaction of the ligand and the receptor in the gas phase is calculated as the sum of ΔE_{ELE} - the electrostatic energy, and ΔE_{VDW} - van der Waals energy. ΔG_{sol} is the free energy of solvation, that is further separated into the non-polar and polar energies. G_{GB} – describes the polar energy of solvation and the generalized Born surface area model is used for its determination. The value of the non-polar solvation energy is calculated based on the surface area that is accessible by solvent. ΔG_{Surf} represents the surface area accessible by the solvent and is used to determine the non-polar energy (Zhang et al., 2017). Docking scores and energy values were used in ranking the ligands and docking poses, with a lower score meaning better affinity.

The hops compounds and flumazenil were docked at the α_1+/γ_2- site (the experimental flumazenil binding site) and the α_1+/β_2- , β_2-/γ_2+ binding pockets of the $\alpha_1\beta_2\gamma_2$ $GABA_AR$ crystal structure (PDB ID: 6D6U). Additionally, CGS-9895 was docked at the α_1+/β_2- pocket. The α_1+/γ_2- binding site is formed by Phe100, His102, Tyr160, Ser205, Ser206, Thr207, Tyr210 (α_1 subunit) and Tyr58, Phe77, Ala79, Thr142 (γ_2 subunit). Residues that form the α_1+/β_2- pocket are Phe100, His102, Tyr160, Ser205, Ser206, Thr207, Tyr210 (α_1 subunit) and Asp43, Tyr62, Gln64 ($\beta2$ subunit). The $\beta2-/\gamma2+$ binding

pocket residues are Asp43, Tyr62, Gln64 (β_2 subunit) and Phe112, Arg114, Tyr72, Thr215, Thr217, Ser217 (γ_2 subunit). The docking site was defined as the centroid of the selected residues with the maximum length of the docked ligands set to 20 Å. The α_1+/β_2- and β_2-/γ_2+ binding site residues at the $\alpha_1\beta_2\gamma_2$ isoform structure were selected based on the article by Zhu et al. (2018). In the $\alpha_6\beta_3\delta$ isoform binding sites model as well as the full receptor model the ligands were docked at the same sites as in the $\alpha_1\beta_2\gamma_2$ crystal structure (Figure 17). Another two docking sites that were probed were the two α_1-/β_3+ sites of the $\alpha_1\beta_3\gamma_2$ isoform crystal structure (PDB ID: 6HUK) (Figure 20). They are the experimentally determined binding pockets of bicuculline (ref). The co-crystallized bicuculline was set as the centroid for the docking pocket and maximum size of the docked ligands was limited to 20 Å.

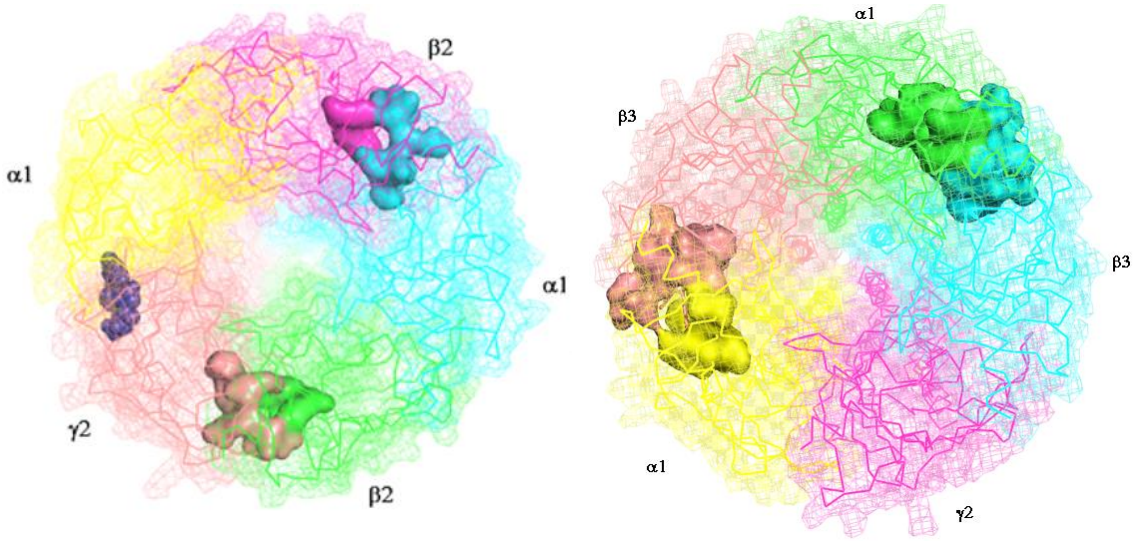

Figure 20. Docking sites at the crystal structures of $\alpha_1\beta_2\gamma_2$ (left) and $\alpha_1\beta_3\gamma_2$ (right) crystal receptor structures (PDB ID: 6D6U, 6HUK, respectively) denoted by the surface presentation of the binding site residues.

5. Acknowledgments

This work was performed in the Pharmaceutical Sciences Laboratory (Pharmacy)/Structural Bioinformatics Laboratory (Biochemistry), at the Åbo Akademi University (ÅAU), Faculty of Science and Engineering.

Hereby, I would like to thank the people who contributed to the success of my thesis:

Prof. (p.t.) Outi Salo-Ahen, PhD (ÅAU, Pharmaceutical Sciences), my scientific supervisor, for providing excellent guidance and support and giving me the opportunity to be a part of her group.

Special thanks to the Head of our Studies, University Teacher Sanna Soini, PhD for all the help and support during my studies and introducing me into the complexity of work that involves $GABA_AR$;

Senior Advisor Prof. Markku Koulu for general introduction to the DDD programme and for advice and guidance during my studies.

Mr. Ali Benkherouf, PhD candidate at the Institute of Biomedicine, University of Turku, for teaching me the basics of working with the cell lines and continuous suggestions and discussions on the thesis results.

All my fellow students, colleagues and friends and, most of all, my family for providing help, encouragement and enabling this study experience for me.

6. List of abbreviations

6PN	6-prenylnaringenin
8PN	8-prenylnaringenin
Ala	Alanine
Arg	Arginine
Asp	Aspartic acid
BZD	Benzodiazepine
Cl^-	Chloride ion
CNS	Central nervous system
D/E	Chains D/E interface
ECD	Extracellular domain
GABA	γ-amino butyric acid
$GABA_AR$	γ-amino butyric acid receptor, class A
$GABA_ARs$	γ-amino butyric acid receptorS, class A
Glu	Glutamic acid
His	Histidine
IXN	Isoxanthohumol
Leu	Leucine
Lys	Lysine
MD	Molecular dynamics
MMGBSA	Molecular Mechanics Generalized Born Surface Area
PDB	Protein Data Bank
Phe	Phenylalanine
Ser	Serine
Thr	Threonine
Tyr	Tyrosine
VMD	Visual Molecular Dynamics

XN	Xanthohumol

7. References

1. ALTSCHUL, S.F., GISH, W., MILLER, W., MYERS, E.W. and LIPMAN, D.J., 1990. Basic local alignment search tool. *Journal of Molecular Biology,* **215**(3), pp. 403-410.

2. AOSHIMA, H., TAKEDA, K., OKITA, Y., HOSSAIN, S.J., KODA, H. and KISO, Y., 2006. Effects of beer and hop on ionotropic gamma-aminobutyric acid receptors. *Journal of Agricultural and Food Chemistry,* 54(7), pp. 2514-2519.

3. AVALLONE, R., ZANOLI, P., PUIA, G., KLEINSCHNITZ, M., SCHREIER, P. and BARALDI, M., 2000. Pharmacological profile of apigenin, a flavonoid isolated from Matricaria chamomilla. *Biochemical Pharmacology,* 59(11), pp. 1387-1394.

4. BAUER, M.R., IBRAHIM, T.M., VOGEL, S.M. and BOECKLER, F.M., 2013. Evaluation and Optimization of Virtual Screening Workflows with DEKOIS 2.0 – A Public Library of Challenging Docking Benchmark Sets. *Journal of Chemical Information and Modeling,* **53**(6), pp. 1447-1462.

5. BAUMANN, S.W., BAUR, R. and SIGEL, E., 2001. Subunit Arrangement of γ-Aminobutyric Acid Type A Receptors. *The Journal of biological chemistry,* **276**(39), pp. 36275-36280.

6. BELINDA J. HALL, MARY CHEBIB, JANE R. HANRAHAN and GRAHAM A.R. JOHNSTON, 2004. Flumazenil-independent positive modulation of g-aminobutyric acid action by 6-methylflavone at human recombinant a1h2g2L and a1h2 GABAA receptors.

7. BENKHEROUF, A.Y., SOINI, S.L., STOMPOR, M. and UUSI-OUKARI, M., 2019. Positive allosteric modulation of native and recombinant GABA A receptors by hops prenylflavonoids. *European journal of pharmacology,* 852, pp. 34.

8. BERMAN, H. M., WESTBROOK, J., FENG, Z., GILLILAND, G., BHAT, T. N., WEISSIG, H., BOURNE, P. E. (2000). The Protein Data Bank. *Nucleic Acids Research*, *28*(1), 235–242.

9. BRAUN, W. and GO, N., 1985. Calculation of protein conformations by proton-proton distance constraints. A new efficient algorithm. *Journal of Molecular Biology,* **186**(3), pp. 611-626.

10. BUHR, A., BAUR, R., MALHERBE, P. and SIGEL, E., 1996. Point mutations of the alpha 1 beta 2 gamma 2 gamma-aminobutyric acid(A) receptor affecting modulation of the channel by ligands of the benzodiazepine binding site. *Molecular Pharmacology,* **49**(6), pp. 1080-1084.

11. CHEN, Y., 2015. Beware of docking! *Trends in Pharmacological Sciences,* **36**(2), pp. 78-95

12. CLAYTON, T., CHEN, J.L., ERNST, M., RICHTER, L., CROMER, B.A., MORTON, C.J., NG, H., KACZOROWSKI, C.C., HELMSTETTER, F.J., FURTMULLER, R., ECKER, G., PARKER, M.W. and COOK, W. SIEGHART

AND J. M., /10/31, 2007-last update, An Updated Unified Pharmacophore Model of the Benzodiazepine Binding Site on γ-Aminobutyric Acida Receptors: Correlation with Comparative Models. Available: http://www.eurekaselect.com/60086/article [May 4, 2019].

13. CLORE, G.M., BRÜNGER, A.T., KARPLUS, M. and GRONENBORN, A.M., 1986. Application of molecular dynamics with interproton distance restraints to three-dimensional protein structure determination: A model study of crambin. *Journal of Molecular Biology,* **191**(3), pp. 523-551.

14. COSSART, R., BERNARD, C. and BEN-ARI, Y., 2005. Multiple facets of GABAergic neurons and synapses: multiple fates of GABA signalling in epilepsies. *Trends in Neurosciences,* **28**(2), pp. 108-115.

15. DEKERMENDJIAN, K., KAHNBERG, P., WITT, M.R., STERNER, O., NIELSEN, M. and LILJEFORS, T., 1999. Structure-activity relationships and molecular modeling analysis of flavonoids binding to the benzodiazepine site of the rat brain GABA(A) receptor complex. *Journal of medicinal chemistry*, 42(21), pp. 4343-4350

16. DEREK P CLAXTON and ERIC GOUAUX, 2018. Expression and purification of a functional heteromeric GABAA receptor for structural studies. *PloS one,* 13(7), pp. e0201210.

17. ELBER, R., RUYMGAART, A. and HESS, B., 2011. SHAKE parallelization. *The European Physical Journal Special Topics,* **200**(1), pp. 211-223.

18. ERNST, M., BRUCKNER, S., BORESCH, S. and SIEGHART, W., 2005. Comparative Models of GABAA Receptor Extracellular and Transmembrane Domains: Important Insights in Pharmacology and Function. *Molecular Pharmacology,* **68**(5), pp. 1291-1300.

19. FRIESNER, R.A., BANKS, J.L., MURPHY, R.B., HALGREN, T.A., KLICIC, J.J., MAINZ, D.T., REPASKY, M.P., KNOLL, E.H., SHELLEY, M., PERRY, J.K., SHAW, D.E., FRANCIS, P. and SHENKIN, P.S., 2004. Glide: a new approach for rapid, accurate docking and scoring. 1. Method and assessment of docking accuracy. *Journal of Medicinal Chemistry,* **47**(7), pp. 1739-1749.

20. FRIESNER, R.A., MURPHY, R.B., REPASKY, M.P., FRYE, L.L., GREENWOOD, J.R., HALGREN, T.A., SANSCHAGRIN, P.C. and MAINZ, D.T., 2006. Extra Precision Glide: Docking and Scoring Incorporating a Model of Hydrophobic Enclosure for Protein−Ligand Complexes. *Journal of Medicinal Chemistry,* **49**(21), pp. 6177-6196.

21. HANRAHAN, J.R., CHEBIB, M. and JOHNSTON, G.A.R., 2011. Flavonoid modulation of GABAA receptors. *British Journal of Pharmacology,* **163**(2), pp. 234-245.

22. HUANG, Q., HE, X., MA, C., LIU, R., YU, S., DAYER, C.A., WENGER, G.R., MCKERNAN, R. and COOK, J.M., 2000. Pharmacophore/Receptor Models for GABAA/BzR Subtypes (α1β3γ2, α5β3γ2, and α6β3γ2) via a Comprehensive Ligand-Mapping Approach. *Journal of Medicinal Chemistry,* **43**(1), pp. 71-95.

23. HUANG, X., LIU, T., GU, J., LUO, X., JI, R., CAO, Y., XUE, H., WONG, J.T., WONG, B.L., PEI, G., JIANG, H. and CHEN, K., 2001. 3D-QSAR Model of Flavonoids Binding at Benzodiazepine Site in GABAA Receptors. *Journal of Medicinal Chemistry,* 44(12), pp. 1883-1891.

24. H XUE, R CHU, J HANG, P LEE and H ZHENG, 1998. Fragment of GABA(A) receptor containing key ligand-binding residues overexpressed in Escherichia coli. *Protein science: a publication of the Protein Society,* **7**(1), pp. 216-219.

25. JACOBSON, M.P., PINCUS, D.L., RAPP, C.S., DAY, T.J.F., HONIG, B., SHAW, D.E. and FRIESNER, R.A., 2004. A hierarchical approach to all-atom protein loop prediction. *Proteins,* **55**(2), pp. 351-367.

26. JACOBSON, M.P., FRIESNER, R.A., XIANG, Z. and HONIG, B., 2002. On the Role of the Crystal Environment in Determining Protein Side-chain Conformations. *Journal of Molecular Biology,* **320**(3), pp. 597-608.

27. JATCZAK-ŚLIWA, M., TEREJKO, K., BRODZKI, M., MICHAŁOWSKI, M.A., CZYZEWSKA, M.M., NOWICKA, J.M., ANDRZEJCZAK, A., SRINIVASAN, R. and MOZRZYMAS, J.W., 2018. Distinct Modulation of Spontaneous and GABA-Evoked Gating by Flurazepam Shapes Cross-Talk Between Agonist-Free and Liganded GABAA Receptor Activity. *Frontiers in Cellular Neuroscience,* **12**, pp. 237.

28. JEREMY P E SPENCER, 2009. Flavonoids and brain health: multiple effects underpinned by common mechanisms. *Genes & nutrition,* **4**(4), pp. 243-250.

29. JOHNSTON, G.A.R., 2015. Flavonoid nutraceuticals and ionotropic receptors for the inhibitory neurotransmitter GABA. *Neurochem.* Int. 89, 120-125.

30. JURSKY, F., FUCHS, K., BUHR, A., TRETTER, V., SIGEL, E. and SIEGHART, W., 2000. Identification of amino acid residues of GABA(A) receptor subunits contributing to the formation and affinity of the tert-butylbicyclophosphorothionate binding site. *Journal of neurochemistry,* **74**, pp. 1310-6.

31. KARABÍN, M., HUDCOVÁ, T., JELÍNEK, L. and DOSTÁLEK, P., 2016. Biologically Active Compounds from Hops and Prospects for Their Use. *Comprehensive Reviews in Food Science and Food Safety,* 15(3), pp. 542-567.

32. KIM, S., CHEN, J., CHENG, T., GINDULYTE, A., HE, J., HE, S., LI, Q., SHOEMAKER, B.A., THIESSEN, P.A., YU, B., ZASLAVSKY, L., ZHANG, J. and BOLTON, E.E., 2019. PubChem 2019 update: improved access to chemical data. *Nucleic Acids Research,* 47(D1), pp. D1109.

33. LI, J., ABEL, R., ZHU, K., CAO, Y., ZHAO, S. and FRIESNER, R.A., 2011. The VSGB 2.0 Model: A Next Generation Energy Model for High Resolution Protein Structure Modeling. *Proteins,* **79**(10), pp. 2794-2812.

34. LI, J., FU, A. and ZHANG, L., 2019. An Overview of Scoring Functions Used for Protein-Ligand Interactions in Molecular Docking. *Interdisciplinary Sciences, Computational Life Sciences*.

35. MACDONALD, R.L., GALLAGHER, M.J., FENG, H. and KANG, J., 2004. GABA(A) receptor epilepsy mutations. *Biochemical Pharmacology,* 68(8), pp. 1497-1506.

36. MACKERELL, A.D., BASHFORD, D., BELLOTT, M., DUNBRACK, R.L., EVANSECK, J.D., FIELD, M.J., FISCHER, S., GAO, J., GUO, H., HA, S., JOSEPH-MCCARTHY, D., KUCHNIR, L., KUCZERA, K., LAU, F.T.K., MATTOS, C., MICHNICK, S., NGO, T., NGUYEN, D.T., PRODHOM, B., REIHER, W.E., ROUX, B., SCHLENKRICH, M., SMITH, J.C., STOTE, R., STRAUB, J., WATANABE, M., WIÓRKIEWICZ-KUCZERA, J., YIN, D. and KARPLUS, M., 1998. All-Atom Empirical Potential for Molecular Modeling and Dynamics Studies of Proteins. *The Journal of Physical Chemistry B,* **102**(18), pp. 3586-3616.

37. MADEIRA, F., PARK, Y.M., LEE, J., BUSO, N., GUR, T., MADHUSOODANAN, N., BASUTKAR, P., TIVEY, A.R.N., POTTER, S.C., FINN, R.D. and LOPEZ, R., 2019. The EMBL-EBI search and sequence analysis tools APIs in 2019. *Nucleic Acids Research.*

38. MAIER, J.A., MARTINEZ, C., KASAVAJHALA, K., WICKSTROM, L., HAUSER, K.E. and SIMMERLING, C., 2015. ff14SB: Improving the Accuracy of Protein Side Chain and Backbone Parameters from ff99SB. *Journal of Chemical Theory and Computation,* **11**(8), pp. 3696-3713.

39. MALDIFASSI, M.C., BAUR, R. and SIGEL, E., 2016. Molecular mode of action of CGS 9895 at α1β2γ2 GABAA receptors. *Journal of neurochemistry,* **138**(5), pp. 722-730.

40. MARTÍ-RENOM, M.A., STUART, A.C., FISER, A., SÁNCHEZ, R., MELO, F. and SALI, A., 2000. Comparative protein structure modeling of genes and genomes. *Annual Review of Biophysics and Biomolecular Structure,* **29**, pp. 291-325.

41. MASIULIS, S., DESAI, R., UCHAŃSKI, T., MARTIN, I.S., LAVERTY, D., KARIA, D., MALINAUSKAS, T., ZIVANOV, J., PARDON, E., KOTECHA, A., STEYAERT, J., MILLER, K.W. and ARICESCU, A.R., 2019. GABA A receptor signaling mechanisms revealed by structural pharmacology. *Nature,* 565(7740), pp. 454-459.

42. MORRIS, A.L., MACARTHUR, M.W., HUTCHINSON, E.G. and THORNTON, J.M., 1992. Stereochemical quality of protein structure coordinates. *Proteins,* **12**(4), pp. 345-364.

43. OLIVEIRA, D.R.D., TODO, A.H., RÊGO, G.M., CERUTTI, J.M., CAVALHEIRO, A.J., RANDO, D.G.G. and CERUTTI, S.M., 2018. *Flavones-bound in benzodiazepine site on GABAA receptor: Concomitant anxiolytic-like and cognitive-enhancing effects produced by Isovitexin and 6-C-glycoside-Diosmetin.*

44. OLSEN, R.W. and DELOREY, T.M., 1999. GABA Receptor Physiology and Pharmacology. *Basic Neurochemistry: Molecular, Cellular and Medical Aspects. 6th edition.* Lippincott-Raven.

45. OLSEN, R.W. and SIEGHART, W., 2009. GABAA receptors: Subtypes provide diversity of function and pharmacology. *Neuropharmacology,* 56(1), pp. 141-148.

46. PAUL S MILLER and A RADU ARICESCU, 2014. Crystal structure of a human GABAA receptor. *Nature,* 512(7514), pp. 270-275.

47. RAMERSTORFER, J., FURTMÜLLER, R., SARTO-JACKSON, I., VARAGIC, Z., SIEGHART, W. and ERNST, M., 2011. The GABAA Receptor α β− Interface: A Novel Target for Subtype Selective Drugs. *Journal of Neuroscience,* **31**(3), pp. 870-877.

48. ROSA COSSART, CHRISTOPHE BERNARD and YEHEZKEL BEN-ARI, 2005. Multiple facets of GABAergic neurons and synapses: Multiple fates of GABA signaling in epilepsies. *Trends in Neurosciences,* 28(2), pp. 108-115.

49. U. RUDOLPH, F. CRESTANI, D. BENKE, I. BRUNIG, J.A. BENSON, J.M. F RITSCHY, J.R. MARTIN, H. BLUETHMANN, H. MOHLER, 1999.Benzodiazepine actions mediated by specific gamma-aminobutyric acid(A) receptor, subtypes. *Nature*, 401 (6755), pp. 796-800.

50. SAHIN, S, EULENBURG, V, KREIS, W, VILLMANN, C. and PISCHETSRIEDER, M. 2016. Three-Step Test System for the Identification of Novel GABAA Receptor Modulating Food Plants. *Plant Foods for Human Nutrition (Dordrecht, Netherlands),* 71(4), pp. 355-360.

51. S.C. LOVELL, I.W. DAVIS, W.B. ARENDALL III, P.I.W. DE BAKKER, J.M. WORD, M.G. PRISANT, J.S. RICHARDSON AND D.C. RICHARDSON (2003) Structure validation by Calpha geometry: phi,psi and Cbeta deviation. *Proteins: Structure, Function & Genetics*. **50**: 437-450.

52. Schrödinger Suite 2019-1 Induced Fit Docking protocol; Glide, Schrödinger, LLC, New York, NY, 2016; Prime, Schrödinger, LLC, New York, NY, 2019.

53. SHEN, M. and SALI, A., 2006. Statistical potential for assessment and prediction of protein structures. *Protein Science,* **15**(11), pp. 2507-2524.

54. SIEGHART, W., 1995. Structure and pharmacology of gamma-aminobutyric acid A receptor subtypes. *Pharmacological Reviews,* 47(2), pp. 181-234.

55. SPENCER, J.P.E., 2008. Flavonoids: modulators of brain function? *The British Journal of Nutrition,* **99 E Suppl 1**, pp. 77.

56. SCIOR T, BENDER A, TRESADERN G, JOSÉ L MEDINA-FRANCO, MARTÍNEZ-MAYORGA K,LANGER T, CUANALO-CONTRERAS K and K AGRAFIOTIS D, 2012. Recognizing Pitfalls in Virtual Screening: A Critical Review. *Journal of Chemical Information and Modeling,* **52**(4), pp. 867-881.

57. SIEVERS F, WILM A, DINEEN DG, GIBSON TJ, KARPLUS K, LI W, LOPEZ R, MCWILLIAM H, REMMERT M, SÖDING J, THOMPSON JD, HIGGINS DG (2011). Fast, scalable generation of high-quality protein multiple sequence alignments using Clustal Omega. *Molecular Systems Biology,* 7(1), pp.

n/a.Clustal Omega [Online]. Available at: http://www.clustal.org/omega/ (Accessed:09 September 2018)

58. SIGEL, E. and ERNST, M., 2018. The Benzodiazepine Binding Sites of GABAA Receptors. *Trends in Pharmacological Sciences,* 39(7), pp. 659-671.

59. SIGEL, E. and STEINMANN, M.E., 2012. Structure, function, and modulation of GABA(A) receptors. *The Journal of biological chemistry,* 287(48), pp. 40224.

60. S RENARD, A OLIVIER, P GRANGER, P AVENET, D GRAHAM, M SEVRIN, P GEORGE and F BESNARD, 1999. Structural Elements of the γ-Aminobutyric Acid Type A Receptor Conferring Subtype Selectivity for Benzodiazepine Site Ligands. *The Journal of biological chemistry,* 274(19), pp. 13370-13374.

61. ŠALI, A. and BLUNDELL, T.L., 1993. Comparative Protein Modelling by Satisfaction of Spatial Restraints. *Journal of Molecular Biology,* **234**(3), pp. 779-815.

62. TRETTER, V., EHYA, N., FUCHS, K. and SIEGHART, W., 1997. Stoichiometry and assembly of a recombinant GABAA receptor subtype. *The Journal of Neuroscience: The Official Journal of the Society for Neuroscience,* **17**(8), pp. 2728-2737.

63. UUSI-OUKARI, M. and KORPI, E.R., 2010. Regulation of GABAA Receptor Subunit Expression by Pharmacological Agents. *Pharmacological Reviews,* **62**(1), pp. 97-135.

64. VARAGIC, Z., WIMMER, L., SCHNÜRCH, M., MIHOVILOVIC, M.D., HUANG, S., RALLAPALLI, S., COOK, J.M., MIRHEYDARI, P., ECKER, G.F., SIEGHART, W. and ERNST, M., 2013. Identification of novel positive allosteric modulators and null modulators at the GABAA receptor α+β− interface. *British Journal of Pharmacology,* **169**(2), pp. 371-383.

65. WEBB, B. and SALI, A., 2014. Comparative Protein Structure Modeling Using MODELLER. *Current Protocols in Bioinformatics,* **47**(1), pp. 5.6.32.

66. WIELAND, H.A., LÜDDENS, H. and SEEBURG, P.H., 1992. A single histidine in GABAA receptors is essential for benzodiazepine agonist binding. *Journal of Biological Chemistry,* **267**, pp. 1426-1429.

67. XIAOHUA ZHANG, HORACIO PEREZ-SANCHEZ and FELICE C. LIGHTSTONE, 2017. A Comprehensive Docking and MM/GBSA Rescoring Study of Ligand Recognition upon Binding Antithrombin. *Current Topics in Medicinal Chemistry,* **17**(14), pp. 1631-1639.

68. XUE, H., ZHENG, H., LI, H.M., KITMITTO, A., ZHU, H., LEE, P. and HOLZENBURG, A., 2000. A fragment of recombinant GABA(A) receptor alpha1 subunit forming rosette-like homo-oligomers. *Journal of Molecular Biology,* **296**(3), pp. 739-742.

69. YAKOUB, K., JUNG, S., SATTLER, C., DAMEROW, H., WEBER, J., KRETZSCHMANN, A., CANKAYA, A.S., PIEL, M., RÖSCH, F.,

HAUGAARD, A.S., FRØLUND, B., SCHIRMEISTER, T. and LÜDDENS, H., 2018. Structure-Function Evaluation of Imidazopyridine Derivatives Selective for δ-Subunit-Containing γ-Aminobutyric Acid Type A (GABAA) Receptors. *Journal of Medicinal Chemistry,* 61(5), pp. 1951-1968.

70. YOCUM, G.T., GALLOS, G., ZHANG, Y., JAHAN, R., STEPHEN, M.R., VARAGIC, Z., PUTHENKALAM, R., ERNST, M., COOK, J.M. and EMALA, C.W., 2016. Targeting the γ-Aminobutyric Acid A Receptor α4 Subunit in Airway Smooth Muscle to Alleviate Bronchoconstriction. *American journal of respiratory cell and molecular biology,* 54(4), pp. 546-553.

71. ZANOLI, P. and ZAVATTI, M., 2008. Pharmacognostic and pharmacological profile of Humulus lupulus L. *Journal of Ethnopharmacology,* 116(3), pp. 383-396.

72. ZHU, S., NOVIELLO, C.M., TENG, J., WALSH, R.M., KIM, J.J. and HIBBS, R.E., 2018. Structure of a human synaptic GABA A receptor. *Nature,* 559(7712), pp. 67-72.

8.Appendix

Graphical and alignment representations of the BLAST similarity search results for the $GABA_AR$ subunits α_6 and δ; a) and b), respectively.

a)

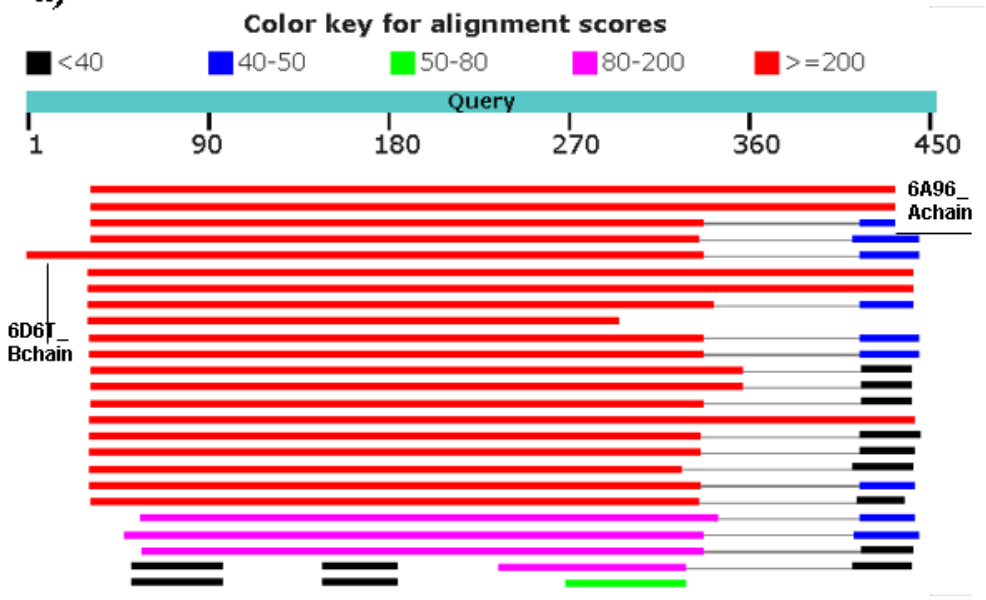

Chain A, Gamma-aminobutyric acid receptor subunit alpha-5,Gamma-aminobutyric acid receptor subunit alpha-5 [Homo sapiens]
Sequence ID: 6A96_A Length: 392 Number of Matches: 2

Range 1: 11 to 354 GenPept Graphics ▼ Next Match ▲ Previous Match

Score	Expect	Method	Identities	Positives	Gaps
473 bits(1218)	5e-166	Compositional matrix adjust.	234/344(68%)	275/344(79%)	7/344(2%)

```
Query  1    MASSLPWLCIILWLENALG-------KLEVEGNFYSENVSRILDNLLEGYDNRLRPGFGG  53
            M  +L   CI + L +  G         ++ E N       +RILD LL+GYDNRLRPG G
Sbjct  11   MIKNLLLFCISMNLSSHFGFSQMPTSSVKDETNDNITIFTRILDGLLDGYDNRLRPGLGE  70

Query  54   AVTEVKTDIYVTSFGPVSDVEMEYTMDVFFRQTWTDERLKFGGPTEILSLNNLMVSKIWT  113
             +T+V+TDIYVTSFGPVSD EMEYT+DVFFRQ+W DERL+F GP + L LNNL+ SKIWT
Sbjct  71   RITQVRTDIYVTSFGPVSDTEMEYTIDVFFRQSWKDERLRFKGPMQRLPLNNLLASKIWT  130

Query  114  PDTFFRNGKKSIAHNMTTPNKLFRIMQNGTILYTMRLTINADCPMRLVNFPMDGHACPLK  173
            PDTFF NGKKSIAHNMTTPNKL R+  +GT+LYTMRLTI+A+CPM+L +FPMD HACPLK
Sbjct  131  PDTFFHNGKKSIAHNMTTPNKLLRLEDDGTLLYTMRLTISAECPMQLEDFPMDAHACPLK  190

Query  174  FGSYAYPKSEIIYTWKKGPLYSVEVPEESSSLLQYDLIGQTVSSETIKSNTGEYVIMTVY  233
            FGSYAYP SE++Y W  G   SV V E+ S L QY L+GQTV +E I ++TGEY IMT +
Sbjct  191  FGSYAYPNSEVVYVWTNGSTKSVVVAEDGSRLNQYHLMGQTVGTENISTSTGEYTIMTAH  250

Query  234  FHLQRKMGYFMIQIYTPCIMTVILSQVSFWINKESVPARTVPGITTVLTMTTLSISARHS  293
            FHL+RK+GYF+IQ Y PCIMTVILSQVSFW+N+ESVPARTVPG+TTVLTMTTLSISAR+S
Sbjct  251  FHLKRKIGYFVIQTYLPCIMTVILSQVSFWLNRESVPARTVPGVTTVLTMTTLSISARNS  310

Query  294  LPKVSYATAMDWFIAVCFAFVFSALIEFAAVNYFTNLQTQKAKR  337
            LPKV+YATAMDWFIAVC+AFVFSALIEFA VNYFT  Q  +A +
Sbjct  311  LPKVAYATAMDWFIAVCYAFVFSALIEFATVNYFTKSQPARAAK  354
```

Range 2: 353 to 382 GenPept Graphics ▼ Next Match ▲ Previous Match ▲ First Match

Score	Expect	Method	Identities	Positives	Gaps
45.4 bits(106)	9e-05	Compositional matrix adjust.	18/30(60%)	24/30(80%)	0/30(0%)

```
Query  415  SKIDQYSRILFPVAFAGFNLVYWVVYLSKD  444
            +KID+ SRI+FPV F  FNLVYW  YL+++
Sbjct  353  AKIDKMSRIVFPVLFGTFNLVYWATYLNRE  382
```

Chain B, Gamma-aminobutyric acid receptor subunit alpha-1,Gamma-aminobutyric acid receptor subunit alpha-1 [Homo sapiens]

Sequence ID: 6D6T_B **Length:** 358 **Number of Matches:** 2

▶See 3 more title(s)

Range 1: 16 to 320 GenPept Graphics ▼Next Match ▲Previous Match

Score	Expect	Method	Identities	Positives	Gaps
475 bits(1222)	3e-167	Compositional matrix adjust.	226/305(74%)	263/305(86%)	0/305(0%)

```
Query  33   SRILDNLLEGYDNRLRPGFGGAVTEVKTDIYVTSFGPVSDVEMEYTMDVFFRQTWTDERL  92
            +RILD LL+GYDNRLRPG G  VTEVKTDI+VTSFGPVSD +MEYT+DVFFRQ+W DERL
Sbjct  16   TRILDRLLDGYDNRLRPGLGERVTEVKTDIFVTSFGPVSDHDMEYTIDVFFRQSWKDERL  75

Query  93   KFGGPTEILSLNNLMVSKIWTPDTFFRNGKKSIAHNMTTPNKLFRIMQNGTILYTMRLTI  152
            KF GP  +L LNNLM SKIWTPDTFF NGKKS+AHNMT PNKL RI ++GT+LYTMRLT+
Sbjct  76   KFKGPMTVLRLNNLMASKIWTPDTFFHNGKKSVAHNMTMPNKLLRITEDGTLLYTMRLTV  135

Query  153  NADCPMRLVNFPMDGHACPLKFGSYAYPKSEIIYTWKKGPLYSVEVPEESSSLLQYDLIG  212
             A+CPM L +FPMD HACPLKFGSYAY ++E++Y W + P  SV V E+ S L QYDL+G
Sbjct  136  RAECPMHLEDFPMDAHACPLKFGSYAYTRAEVVYEWTREPARSVVVAEDGSRLNQYDLLG  195

Query  213  QTVSSETIKSNTGEYVIMTVYFHLQRKMGYFMIQIYTPCIMTVILSQVSFWINKESVPAR  272
            QTV S  ++S+TGEYV+MT +FHL+RK+GYF+IQ Y PCIMTVILSQVSFW+N+ESVPAR
Sbjct  196  QTVDSGIVQSSTGEYVVMTTHFHLKRKIGYFVIQTYLPCIMTVILSQVSFWLNRESVPAR  255

Query  273  TVFGITTVLTMTTLSISARHSLPKVSYATAMDWFIAVCFAFVFSALIEFAAVNYFTNLQT  332
            TVFG+TTVLTMTTLSISAR+SLPKV+YATAMDWFIAVC+AFVFSALIEFA VNYFT  Q
Sbjct  256  TVFGVTTVLTMTTLSISARNSLPKVAYATAMDWFIAVCYAFVFSALIEFATVNYFTKSQP  315

Query  333  QKAKR  337
             +A +
Sbjct  316  ARAAK  320
```

Range 2: 319 to 348 GenPept Graphics ▼Next Match ▲Previous Match ▲First Match

Score	Expect	Method	Identities	Positives	Gaps
42.7 bits(99)	7e-04	Compositional matrix adjust.	17/30(57%)	23/30(76%)	0/30(0%)

```
Query  415  SKIDQYSRILFPVAFAGFNLVYWVVYLSKD  444
            +KID+ SRI FP+ F  FNLVYW  YL+++
Sbjct  319  AKIDRLSRIAFPLLFGIFNLVYWATYLNRE  348
```

b)

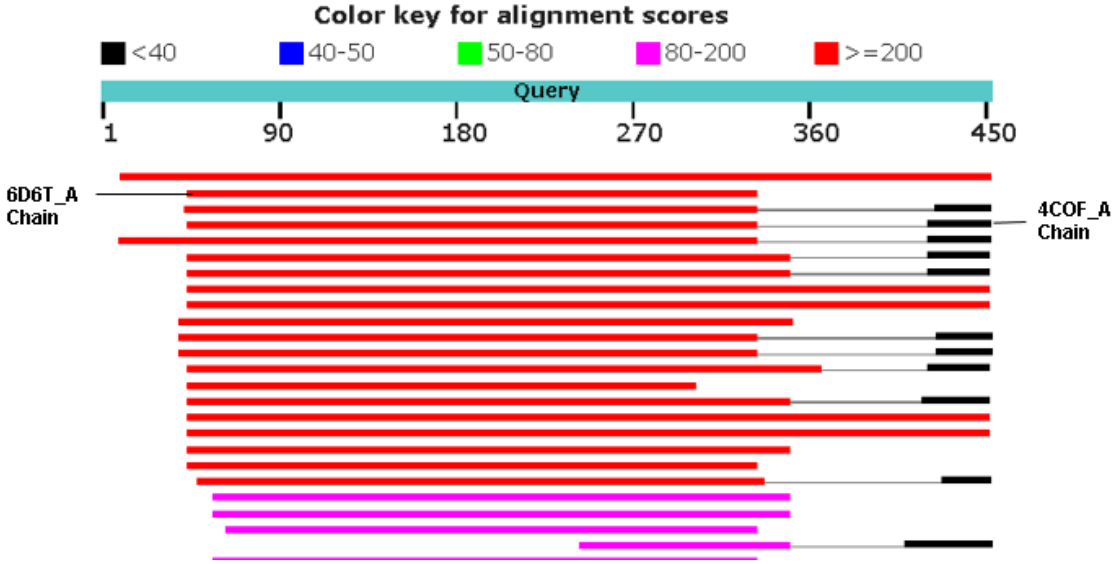

Chain A, Gamma-aminobutyric acid receptor subunit beta-2,Gamma-aminobutyric acid receptor subunit beta-2 [Homo sapiens]

Sequence ID: 6D6T_A **Length:** 341 **Number of Matches:** 1

▶See 3 more title(s)

Range 1: 16 to 304 GenPept Graphics ▼Next Match ▲Previous Match

Score	Expect	Method	Identities	Positives	Gaps
333 bits(854)	1e-111	Compositional matrix adjust.	149/290(51%)	210/290(72%)	1/290(0%)

```
Query  44   LDGLIAGYARNFRPGIGGPPVNVALALEVASIDHISEANMEYTMTVFLHQSWRDSRLSYN  103
            +D L+ GY    RP  GGPPV V + +++ASID +SE NM+YT+T++  Q+WRD RLSYN
Sbjct  16   VDRLLKGYDIRLRPDFGGPPVAVGMNIDIASIDMVSEVNMDYTLTMYFQQAWRDKRLSYN  75

Query  104  HTNETLGLDSRFVDKLWLPDTFIVNAKSAWFHDVTVENKLIRLQPDGVILYSIRITSTVA  163
                 L LD+R  D+LW+PDT+ +N K ++ H VTV+N++IRL PDG +LY +RIT+T A
Sbjct  76   VIPLNLTLDNRVADQLWVPDTYFLNDKKSFVHGVTVKNRMIRLHPDGTVLYGLRITTTAA  135

Query  164  CDMDLAKYPMDEQECMLDLESYGYSSEDIVYYWSESQEHIHGLDKLQLAQFTITSYRFTT  223
            C MDL +YP+DEQ C L++ESYGY+++DI +YW      + G+ K++L QF+I  Y+  T
Sbjct  136  CMMDLRRYPLDEQNCTLEIESYGYTTDDIEFYWRGDDNAVTGVTKIELPQFSIVDYKLIT  195

Query  224  ELMNFKSAGQFPRLSLHFHLRRNRGVYIIQSYMPSVLLVAMSWVSFWISQAAVPARVSLG  283
            + + F S G +PRLSL F L+RN G +I+Q+YMPS+L+  +SWVSFWI+  A  ARV+LG
Sbjct  196  KKVVF-STGSYPRLSLSFKLKRNIGYFILQTYMPSILITILSWVSFWINYDASAARVALG  254

Query  284  ITTVLTMTTLMVSARSSLPRASAIKALDVYFWICYVFVFAALVEYAFAHF  333
            ITTVLTMTT+    R +LP+   +KA+D+Y   C+VFVF AL+EYA  ++
Sbjct  255  ITTVLTMTTINTHLRETLPKIPYVKAIDMYLMGCFVFVFMALLEYALVNY  304
```

Chain A, Gamma-aminobutyric Acid Receptor Subunit Beta-3 [Homo sapiens]

Sequence ID: 4COF_A **Length:** 355 **Number of Matches:** 2

▶See 4 more title(s)

Range 1: 19 to 307 GenPept Graphics ▼Next Match ▲Previous Match

Score	Expect	Method	Identities	Positives	Gaps
328 bits(840)	2e-109	Compositional matrix adjust.	145/290(50%)	211/290(72%)	1/290(0%)

```
Query  44   LDGLIAGYARNFRPGIGGPPVNVALALEVASIDHISEANMEYTMTVFLHQSWRDSRLSYN  103
            +D L+ GY    RP  GGPPV V + +++ASID +SE NM+YT+T++  Q WRD RL+Y+
Sbjct  19   VDKLLKGYDIRLRPDFGGPPVCVGMNIDIASIDMVSEVNMDYTLTMYFQQYWRDKRLAYS  78

Query  104  HTNETLGLDSRFVDKLWLPDTFIVNAKSAWFHDVTVENKLIRLQPDGVILYSIRITSTVA  163
                 L LD+R  D+LW+PDT+ +N K ++ H VTV+N++IRL PDG +LY +RIT+T A
Sbjct  79   GIPLNLTLDNRVADQLWVPDTYFLNDKKSFVHGVTVKNRMIRLHPDGTVLYGLRITTTAA  138

Query  164  CDMDLAKYPMDEQECMLDLESYGYSSEDIVYYWSESQEHIHGLDKLQLAQFTITSYRFTT  223
            C MDL +YP+DEQ C L++ESYGY+++DI +YW    + + G+++++L QF+I  +R  +
Sbjct  139  CMMDLRRYPLDEQNCTLEIESYGYTTDDIEFYWRGGDKAVTGVERIELPQFSIVEHRLVS  198

Query  224  ELMNFKSAGQFPRLSLHFHLRRNRGVYIIQSYMPSVLLVAMSWVSFWISQAAVPARVSLG  283
              + F + G +PRLSL F L+RN G +I+Q+YMPS+L+  +SWVSFWI+  A  ARV+LG
Sbjct  199  RNVVF-ATGAYPRLSLSFRLKRNIGYFILQTYMPSILITILSWVSFWINYDASAARVALG  257

Query  284  ITTVLTMTTLMVSARSSLPRASAIKALDVYFWICYVFVFAALVEYAFAHF  333
            ITTVLTMTT+    R +LP+   +KA+D+Y   C+VFVF AL+EYAF ++
Sbjct  258  ITTVLTMTTINTHLRETLPKIPYVKAIDMYLMGCFVFVFLALLEYAFVNY  307
```